

ABSTRACT

WATSON, KYLE LIVINGSTON. From Radiant Protective Performance to RadMan™: The Role of Clothing Materials in Protecting against Radiant Heat Exposures in Wildland Forest Fires. (Under the direction of Dr. Roger Barker).

Advances in clothing thermal comfort must consider the fundamental need to provide adequate protective insulation against the hazardous heat exposures encountered in wildland fire fighting. This research will review the basis for establishing testing methodologies employed to evaluate the thermal protective performance of fabric materials used in wildland protective gear. The results of this research have developed a new bench-scale testing platform that uses water cooled thermal sensor technology and an advanced skin burn injury model to provide a more accurate prediction for the onset of burn injuries resulting from the transmission of radiant heat. This research also demonstrated the RadMan™ system, a new full-scale instrumented manikin technology developed to measure the radiant heat protection provided by firefighter suits. This systems-level testing approach used by RadMan™ is providing new insights about how different heat resistant fabrics, base layers, and garment fit affect the skin burn protection. The knowledge from this research will be useful to identify and develop clothing materials that offer optimum protective performance against radiant heat exposures encountered in wildland firefighting.

© Copyright 2014 by Kyle Watson

All Rights Reserved

From Radiant Protective Performance to RadMan™: The Role of Clothing Materials in
Protecting against Radiant Heat Exposures in Wildland Forest Fires

by
Kyle Livingston Watson

A thesis submitted to the Graduate Faculty of
North Carolina State University
in partial fulfillment of the
requirements for the degree of
Master of Science

Textile Engineering

Raleigh, North Carolina

2014

APPROVED BY:

Dr. Kirill Efimenko

Dr. Alexander Hummel

Dr. Roger Barker
Committee Chair

BIOGRAPHY

Kyle Livingston Watson was born on July 8th, 1990 to Craig Watson and Amy Day. He grew up in Wilmington, North Carolina where he attended elementary and middle school until graduating from E. A. Laney High School in 2008.

Kyle moved to Raleigh, North Carolina later that year to pursue a degree at North Carolina State University. As an undergraduate student, he studied Textile Engineering with a concentration in Product Development. During this time, he performed undergraduate research in the field of electrospinning. Kyle graduated in the spring of 2012 and immediately began his work on a Master's degree in Textile Engineering at the Textile Protection and Comfort Center (TPACC). Throughout this process he participated in a wildlands firefighting research project with a focus on thermal protection sponsored by FEMA. Kyle will graduate in the spring of 2014 with the Degree of Master of Science in Textile Engineering.

ACKNOWLEDGMENTS

I would like to express my gratitude toward my research advisor Dr. Roger Barker for his advice and knowledge that allowed me to craft the best work possible. I would also like to recognize Dr. Alexander Hummel for his assistance which proved invaluable throughout this entire process. I would like to thank FEMA and the Department of Homeland Security for sponsoring the project in which my research was founded upon. I would also like to thank my peers within the Textile Protection and Comfort Center for their help and input with my research.

TABLE OF CONTENTS

LIST OF TABLES.....	vi
LIST OF FIGURES.....	vii
CHAPTER 1: INTRODUCTION.....	1
1.1 Purpose.....	1
1.2 Research Objectives.....	1
1.3 Need for Research.....	3
1.4 Wildlands Firefighting Environment.....	5
1.5 Burn Injuries.....	6
CHAPTER 2: COMPARISON OF TWO BENCH LEVEL TEST METHODS.....	7
2.1 Introduction.....	7
2.1.1 Comparison of RPP Test Methods.....	9
2.1.2 Burn Prediction Model Comparisons.....	13
2.2 Experimental Procedures.....	18
2.3 Test Procedure Comparison.....	19
2.4 Results and Discussion.....	21
2.4.1 Effect of Test Method in RPP Ratings.....	21
2.4.2 Effect of Heat Exposure Intensity.....	24
2.4.3 Effect of Test Platform Differences.....	26
2.4.4 Effect of Burn Model.....	32
2.4.3 Repeatability Validation of Both Test Methods.....	33
2.4.4 Material Discrimination Experiments.....	34
2.5 Conclusions.....	36
CHAPTER 3: EVALUATION OF WILDLAND FIREFIGHTING MATERIALS.....	37
3.1 Introduction.....	37
3.2 Reasonable Maximum Exposure.....	39
3.3 Wildland Firefighter Garments.....	42
3.4 Experimental.....	43
3.4.1 Test Materials.....	43
3.4.2 Methods.....	44
3.5 Results and Discussion.....	45

3.5.1 Effect of Test Method	50
3.6 Conclusions.....	52
CHAPTER 4: RADMAN™	53
4.1 Introduction.....	53
4.2 Need for Radiant Man.....	54
4.3 RadMan™ Development	57
4.4 Results and Discussions.....	62
4.4.1 RadMan™ Sensor Validation	62
4.4.2 RadMan™ Test Procedure.....	65
4.4.3 Test Materials.....	67
4.5 Results and Discussion	69
4.5.1 Effect of Garment Construction.....	76
4.5.2 Garment Thermal Degradation	78
4.5.3 Correlation between ASTM F 2731 RPP Rating and RadMan™	79
4.6 Conclusions.....	80
CHAPTER 5: CONCLUSIONS AND RECOMMENDATIONS.....	80
5.1 Implications for Future Research.....	82
REFERENCES.....	83
APPENDIX.....	87
A.1 Cumulative to Instantaneous Heat Flux Conversion.....	88
A.2 Significant Difference of ASTM F 1939 and 2731.....	88

LIST OF TABLES

Table 2-1: Working Heat Flux Exposures to Wildland Firefighters in the Field	8
Table 2-2: Comparison of Apparatus Properties	18
Table 2-3: Materials	19
Table 2-4: t Test Comparison of Significant Difference between Test Methods	22
Table 2-5: Burn Model Prediction Comparison.....	32
Table 2-6: Repeatability Study for ASTM F 1939 & ASTM F 2731	33
Table 2-7: Differentiation of Both Test Platforms.....	35
Table 3-1: Test Materials	44
Table 4-1: Bench Level Materials.....	63
Table 4-2: RPP Rating of RadMan™ Sensor vs. ASTM F 2731 Sensor	64
Table 4-3: RadMan™ Materials	68
Appendix Table 1: Statistical Significant Difference Analysis of Both Test Platforms.....	86

LIST OF FIGURES

CHAPTER 2: COMPARISON OF TWO BENCH LEVEL TEST METHODS

Figure 2-1: Wildland Environment Thermal Ranges.....	11
Figure 2-2: ASTM F 1939 (Left) & ASTM F 2731 (Right) Concept & Photographic Comparison.....	13
Figure 2-3: Stoll Curve demonstrating intersection point from sensor heat flux	14
Figure 2-4: 1-D Burn Injury Prediction Model used in ASTM F 2731	16
Figure 2-5: RPP Rating Comparison	22
Figure 2-6: ASTM F 1939 vs. 2731 Correlation.....	23
Figure 2-7: RPP Rating vs. Fabric Weight Test Method Comparison	24
Figure 2-8: Effect of Heat Exposure Intensity in ASTM F 1939 on RPP for Fabric N.....	25
Figure 2-9: Exposure Intensity Degradation Comparison	26
Figure 2-10: Instant Heat Flux Comparison between Water Cooled Sensor in Both Test Platforms at RME Exposure Intensity for Fabric C.....	28
Figure 2-11: Instant Heat Flux Comparison between Copper Sensor in Both Test Platforms at RME Exposure Intensity for Fabric C	29
Figure 2-12: ASTM F 1939 vs. ASTM F 2731 Instant Heat Flux Comparison at RME Exposure Intensity for Fabric E	31

CHAPTER 3: EVALUATION OF WILDLAND FIREFIGHTING MATERIALS

Figure 3- 1: Wildland Environment Thermal Ranges.....	38
Figure 3- 2: Cohen Flame Radiation Model	41
Figure 3- 3: RPP Ratings	46
Figure 3- 4: RPP vs. Weight	48
Figure 3- 5: RPP vs. Thickness.....	49
Figure 3- 6: Comparison of ASTM F 1939 & 2731 RPP vs. Weight.....	50
Figure 3- 7: Degradation of Fabrics when Tested by ASTM F 1939 Method.....	51

CHAPTER 4: RADMAN™

Figure 4- 1: RadMan™ Sensor Locations	58
Figure 4- 2: RadMan™ RdF Foil Sensor.....	59
Figure 4- 3: RadMan™ Articulation.....	60
Figure 4- 4: RadMan™ Output.....	61
Figure 4- 5: RadMan™ Model	62
Figure 4- 6: RadMan™ Heat Flux Distribution.....	66

Figure 4- 7: RadMan™ Dressed in Wildland Fighting PPE.....	68
Figure 4- 8: Garment A Composite Image Time Progression	70
Figure 4- 9: RadMan™ Burn Data for Percentage of Front Body Burns at 60 Second Time Interval	71
Figure 4- 10: RadMan™ Burn Data for Percentage of Front Body Burns at 90 Second Time Interval	72
Figure 4- 11: RadMan™ Burn Data for Percentage of Front Body Burns at 120 Second Time Interval	73
Figure 4- 12: RadMan™ Burn Data for Percentage of Front Body Burns at 150 Second Time Interval	74
Figure 4- 13: Garment Construction Comparison	77
Figure 4- 14: Fabric Degradation after Thermal Exposure.....	78
Figure 4- 15: Bench Level ASTM F 2731 RPP vs. Full Scale Front Body Burn % Comparison.....	79

CHAPTER 1: INTRODUCTION

1.1 Purpose

Wildland firefighters experience a unique situation in their field of work. The primary concern in the past has been to prevent burn injuries first and foremost. However, recent studies are demonstrating that heat stress created from unnecessarily heavy garments is causing more overall injuries than the burns the clothing is designed to insulate the wearer from. A collection of data from the years 1990-2006 shows that more wildland firefighters were killed from heart attacks than burn injuries [1]. With this fact in mind, a shift in priorities of personal protection equipment (PPE) is warranted. Project Aquarius supports this hypothesis by suggesting that the “physical exertion contributed more than twice as much as did fire and weather to the heat load and physiological strain” [2]. The fact that heat stress is a more pressing issue suggests that the garment constructions and thus the standards by which they are evaluated need to be addressed. This issue leads to a vast amount of research being conducted in order to balance the protection and comfort aspects of wildlands protective clothing.

1.2 Research Objectives

The intent of this research is to explore the limitations of the current Radiant Protective Performance (RPP) test method utilized in the evaluation of wildland protective garments as well as provide an alternative method that more accurately portrays the protection gained from the fabric. The materials used within the bench level portion of this

research will then be analyzed by the novel manikin system referred to as RadMan™ which was designed to replicate human response to a radiant heat source. Between both the bench level and garment scale tests performed within this research a more complete understanding of wildland PPE will be achieved.

Objectives of the research include:

1. Critically evaluate the current RPP test method to establish its validity in the application of wildland fabric testing
2. Improve upon the aforementioned test method's deficiencies and limitations to provide increased realism in protection results
3. Investigate the effect of heat exposure intensity on FR fabrics and base layers used in PPE for wildland firefighters' clothing ensembles
4. Demonstrate a systems level test method for evaluating the radiant protective performance of wildland firefighter clothing

Completion of these objectives will ensure the most accurate fabric response to radiant heat which will potentially open the door for lighter weight fabrics that provide the same protection that the previous test methodology was unable to account for. It may also provide additional perspective on the differences between basic fabric testing and the full garments worn in practice. This perspective should impart critical knowledge on what improvements can be made to the garments as well as to where they should be implemented.

1.3 Need for Research

An investigation from 1990-2006 established that 21.9% of wildlands firefighter deaths resulted from heart attacks which were the 3rd leading culprit with aircraft and vehicle accidents slightly ahead of it with 23.2% and 22.9% respectively. Heart attacks were typically observed in volunteer firefighters that were not required to participate in a fitness or health exam. The build-up of metabolic heat within the body that has been trapped within from the protective garments creates an immense amount of stress on the heart creating severe problems. In addition, heat stress accounted for approximately three percent of casualties on its own. Deaths caused by burn over situations ranked 4th and caused 20.6% of fatalities [1]. A burn-over occurrence transpires when a fire spreads too rapidly for the firefighter to escape and must deploy their fire shelter in the attempt to protect themselves from the approaching flames. Fire shelters are tent like structures composed of high insulating foil designed to shield the worker in a last line of defense [3]. Although the shelter generally provides adequate protection against the physical flames and radiant heat, it cannot prevent the inhalation of the extremely hot air that is emanating from the fire. For this reason, no practical amount of PPE could prevent against an injury or death.

On June 30th 2013, nineteen Arizona Hotshot wildland firefighters were killed in the line of duty when caught in a burn-over scenario. Hotshots are an elite crew usually comprised of 20 workers that are the first on scene that clear the surrounding area of any combustible material in the attempt to contain the raging fire. In this particular situation, a swift change in wind direction on a day with dry ground and low humidity caused the flames

to surround the men too quickly and they were forced to deploy their fire shelters in a last ditch attempt to protect themselves. Unfortunately, the fire did not pass over them quickly enough and all were killed except for one member who was tasked with the “lookout” position and managed to escape after warning his coworkers of the approaching danger [4]. This was the deadliest day for firefighters since the 9/11 attacks in 2001. This specific event is one of many that demonstrate that even the most protective of measures is unable to fully defend against the absolute worst that nature has to offer. The goal of protection should be to provide a garment that defends against the vast majority of realistic and dangerous scenarios while still providing an improvement in the release of metabolic heat so that heat stress and the resulting fatigue do not affect a firefighter’s judgment. Project Aquarius suggests that physical exertion accounted for 71% of the heat load that the firefighter experienced while weather and fire comprised the rest [5]. Ideally, this will decrease the number of burn-over situations that the workers put themselves in.

Before firefighters even consider approaching a fire, they are trained to estimate a safety zone distance from the physical flames in order to allot themselves enough time to escape or if the situation calls for it, deploy their fire shelter. The general rule is to stand approximately four times the flame height away from the base of the fire. This distance ensures that an additional thermal danger such as convective heating which is only an issue in close proximity to the fire is removed from the equation as much as possible. Instead, radiant heat is the primary hazard [6]. It is this thermal energy that research has focused upon to safeguard against.

1.4 Wildlands Firefighting Environment

The hottest of wildlands fires, known as crown fires, can be observed to possess radiant heat fluxes upwards of 40 kW m^{-2} with air temperatures of $300 \text{ }^\circ\text{C}$ two meters away. The more common bushfire, which can be managed with a hand-tool crew, comes nowhere close to these extreme conditions except in burn-over situations. A series of experiments performed in Project Aquarius in Australia where brush fires were purposefully lit in order to gather valuable information about the environment. The average conditions were as follows; air temperature of $25 \text{ }^\circ\text{C}$ with a range of $17\text{-}33 \text{ }^\circ\text{C}$, relative humidity average of 47% with a range of $14\text{-}81 \%$, and a wind speed average of 4.4 m s^{-1} with a range of $2\text{-}9 \text{ m s}^{-1}$. The recorded radiant fluxes were from $0.5\text{-}8.6 \text{ kW m}^{-2}$ but were most commonly 1.6 kW m^{-2} [5]. This same study on brush fires demonstrated that with different combinations of flame height ranging from 0.3 to 1.2 m , height above the ground from 0.6 to 0.9 m , and distance from flames ranging from 0.6 to 1.8 m ; they found that the radiant heat flux varied within the region of 0.4 to 4.6 kW m^{-2} . A separate experiment showed that the maximum heat flux a firefighter might experience from a wildfire was approximately 8.6 kW m^{-2} . It was also found that with any heat flux below 2.0 kW m^{-2} , no pain was experienced.

The study that propelled the work done in this research is referred to as the “Wildland Fire Fighting Hazard & Risk Assessment” which was performed by the California Department of Forestry & Fire Protection (CAL FIRE) [7]. This particular study employed the use of Jack D. Cohen’s flame radiation model which enabled the estimation of a typical fire that wildland firefighters might experience in the field [8].

Cohen's heat radiation model is based upon a "worst case scenario" as is evidenced by the flame hedge shape geometry that is selected. Fires do not typically exist in this form; they are always shifting and dynamic. By defining the flames in this particular way, the model predicts the absolute maximum heat flux that could be potentially achieved by the fire. The flame wall is simplified down to the essence of two centered and rectangular parallel plates with one side representing the fire and the other as the area that is absorbing the radiant heat. This estimation allows us to calculate a "Reasonable Maximum Exposure" (RME) in which firefighters can expect to experience except in extraordinary and rare occurrences. It is this Reasonable Maximum Exposure flux in which this research will focus upon.

1.5 Burn Injuries

A major concern of firefighters when working in the field is the near constant threat of thermal dangers that can generate burn injuries. There are four types of burn injuries that exist. A first degree burn occurs only at the outer layer of skin referred to as the epidermis and is the most common and minor of them all. A second degree burn is more severe and involves the destruction of the epidermis and the partial damage of the second layer of skin called the dermis. Second degree burns are considered minor if it covers less than 15% of the body [9]. It is this type of burn that researchers try to replicate in order to attempt to prevent against it in future real-life situations. A third degree burn involves the destruction of all three layers of skin, will most likely never heal completely and is potentially fatal. Finally, a fourth degree burn will occur if the burn extends into the muscle or bone. This rare type of

burn is often found in electrical burn situations [10]. It is the second degree burn in which this research has focused upon as a bench mark of radiant thermal protection.

CHAPTER 2: COMPARISON OF TWO BENCH LEVEL TEST METHODS

2.1 Introduction

The Radiant Protective Performance (RPP) test is the standard test method for evaluating the thermal protective performance of protective clothing materials in radiant heat exposures. The American Society for Testing and Materials (ASTM) standard F 1939 [11] describes the “Standard Test Method for Radiant Heat Resistance of Flame Resistant Clothing Materials with Continues Heating” and specifies the test apparatus to be used for fabric testing. This test method is referenced in a number of National Fire Protection Association (NFPA) standards, such as 1971 [12], 2112 [13], and 1977 [14]. These NFPA standards define RPP performance criteria needed to certify the flame resistant fabrics and garments used for structural firefighting, industrial coveralls, and wildland firefighting garments, respectively.

The ASTM F 1939 apparatus and test method used to predict RPP have remained relatively unchanged for decades and were originally developed to replicate high intensity (84 kW m^{-2}), short duration (< 10 seconds) heat exposures, specifically for structural firefighting clothing. NFPA 1977 [14] (for wildland firefighters) has adopted a lower level of heat exposure of 21 kW m^{-2} , resulting in longer duration testing times. Though 21 kW m^{-2} is one quarter of the exposure flux of the original RPP test, recent research (Table 2-1) has

shown that this is still significantly too high to represent realistic working conditions for daily wildland firefighting.

Table 2-1: Working Heat Flux Exposures to Wildland Firefighters in the Field

Author	Maximum Heat Exposure to Firefighter	Method for obtaining data
CAL FIRE [7]	RME = 7.1 kW m ⁻²	Cohen fire wall thermal modeling [8]
Project Aquarius 4 [15]	8.6 kW m ⁻² with an average of less than 2 kW m ⁻²	Experimental fires were lit and then measured with a series of radiometers
Phani K. Raj [16]	6.3 kW m ⁻² with an average of 5 kW m ⁻²	Measured flux of liquefied natural gas fire from a range of distances
Sullivan, Ellis, Knight [17]	6.7 kW m ⁻²	Stephan-Boltzmann thermal radiation model
Packham & Pompe [18]	6.3 kW m ⁻²	Estimation of view factor and measurement of fire intensity via radiometer

The findings from the five independent projects from Table 2-1 describe the highest heat flux experienced by wildland firefighters in the field is approximately between 6.3-8.6 kW m⁻², which is significantly less than the 21 kW m⁻² currently used by the RPP test method in NFPA 1977 [14]. The most recent project, conducted by the California Department of Forestry and Fire Protection (CAL FIRE), defined a “Reasonable Maximum Exposure” (RME) for wildland firefighting to be equivalent to 7.1 kW/m². This RME value was found through modeling of a flame wall (Cohen Model [8]) and based off the traditional “hauling

chart” [19] that wildland firefighters use to determine their safe operating distance from a fire based on flame height. This RME value is a good reference point for reduction in RPP heat flux intensity and will be used for this study.

The NFPA 1977 standard employs a minimum criterion RPP value of 7 that must be reached before a prospective fabric can be certified. This RPP value is attained by accounting for time to 2nd degree burn and incident heat flux and will be further explained later. The RPP value of 7 was selected due to the fact that the currently worn 7.7 oz yd⁻² green meta-aramid pants passed this criterion. CAL FIRE approached the RPP criteria selection from an alternative point of view and determined that the minimum PPE fabric should provide protection for at least 60 seconds which supplies an RPP rating of 10. The basis for the CAL FIRE rating provides an improved logical thought process instead of utilizing a value that passes current fabrics for simplicity.

Though reducing the output heat flux intensity for RPP is relatively simple to do, the original apparatus and sensors were designed for high intensity, short duration exposures, making them insufficient for low intensity, long duration exposures. The purpose of this research study is to identify an optimum test methodology for evaluating the RPP of wildland firefighter clothing materials at RME intensity.

2.1.1 Comparison of RPP Test Methods

Two standardized test methods are available for measuring the radiant protective performance (RPP) of protective clothing materials. ASTM F 1939 exposes a fabric sample to a predetermined level of radiant energy and measure the amount of heat passing through

the barrier fabric to a sensor (representing human skin beneath clothing). The basic elements of the RPP test apparatus consists of the heat source, heat flux sensor, specimen holder, heat shield, and data acquisition system. The standard heating source is a bank of five 500 W infrared radiant quartz tubes positioned 25.4 ± 0.4 mm from the fabric sample surface. The sensor is a copper calorimeter that provides both temperature and heat flux information to the data acquisition system which interprets this data into a burn injury prediction using the Stoll Curve [20].

ASTM F 1939 is currently a widely accepted test platform that has been specified as the test of choice for radiant heat protection in NFPA 1977. The test methodology was originally developed for the evaluation of protection gained by aluminized fabrics. However, research into the intricacies of the test platform has revealed potential issues such as the presence of heat saturation present within the copper calorimeter sensor [21]. The test platform was originally designed for high intensity exposures for short durations in which heat saturation is not normally an issue. The proposed reduction to RME intensity lengthens the test exposure times creating potential heat saturation complications.

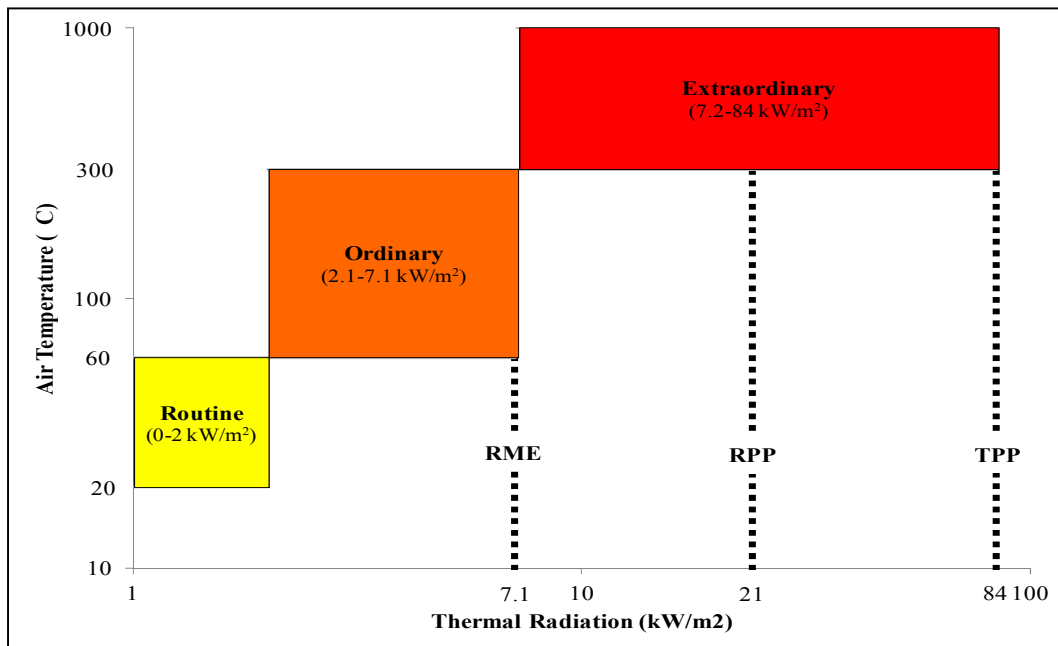


Figure 2-1: Wildland Environment Thermal Ranges

The study performed by CAL FIRE [7] has also brought into question the reproducibility of the ASTM F 1939 test platform between labs. In that research, it became clear that no two labs were able to attain similar second degree burn times; most likely a result of variation between lab conditions, equipment, and operator.

The test apparatus from ASTM F 2731 [22] is the proposed new RPP device and is based off of the platform specifically developed for evaluating transmitted and stored thermal energy in longer duration radiant heat exposures by North Carolina State University and Measurement Technologies Northwest [23]. The elements of the ASTM F 2731 test apparatus are similar to the ASTM F 1939 device and consist of a heat source, heat flux

sensor, specimen holder, and data acquisition system. The apparatus differs from the standard RPP by including a water cooled sensor block to replicate the constant temperature and blood flow effects of human skin and an automated shutter system to reduce human operator variation in the test platform. The sensor is a water cooled Schmidt-Boelter thermopile sensor and housing, set to a human skin temperature of 32.5 °C which eliminates the heat saturation of the standard copper calorimeter used by ASTM F 1939 and improves the accuracy of testing over longer durations. The water cooled sensor and housing is also ideally a better skin simulant than its ASTM F 1939 copper slug and ceramic insulating block counterpart due to replication of blood flow. The heat source used is a ceramic black body simulator which provides a very consistent and improved exposure flux. It replicates the wave form of actual fires and utilizes control feedback that enables the system to maintain steadier flux outputs as opposed to the constant energy output of ASTM F 1939. The heat source is positioned 108 ± 5 mm from the sample holder. The spacing holder plate has also been modified to 0.09 inches between fabric and sensor in order to directly compare to results obtained from ASTM F 1939 experiments. The heat flux has been altered from the suggested 8.5 kW m^{-2} in ASTM F 2731 to the 7.1 kW m^{-2} RME flux. It has been demonstrated that ASTM F 2731 provides excellent reproducibility due to the automated functions such as transfer tray movement and controlled power feedback [23]. For the purposes of the experiments performed in this study, the compression portion and moisture conditioning present in ASTM F 2731 have been removed as those apply to the stored energy aspects of a fabric which is not a factor in this research.

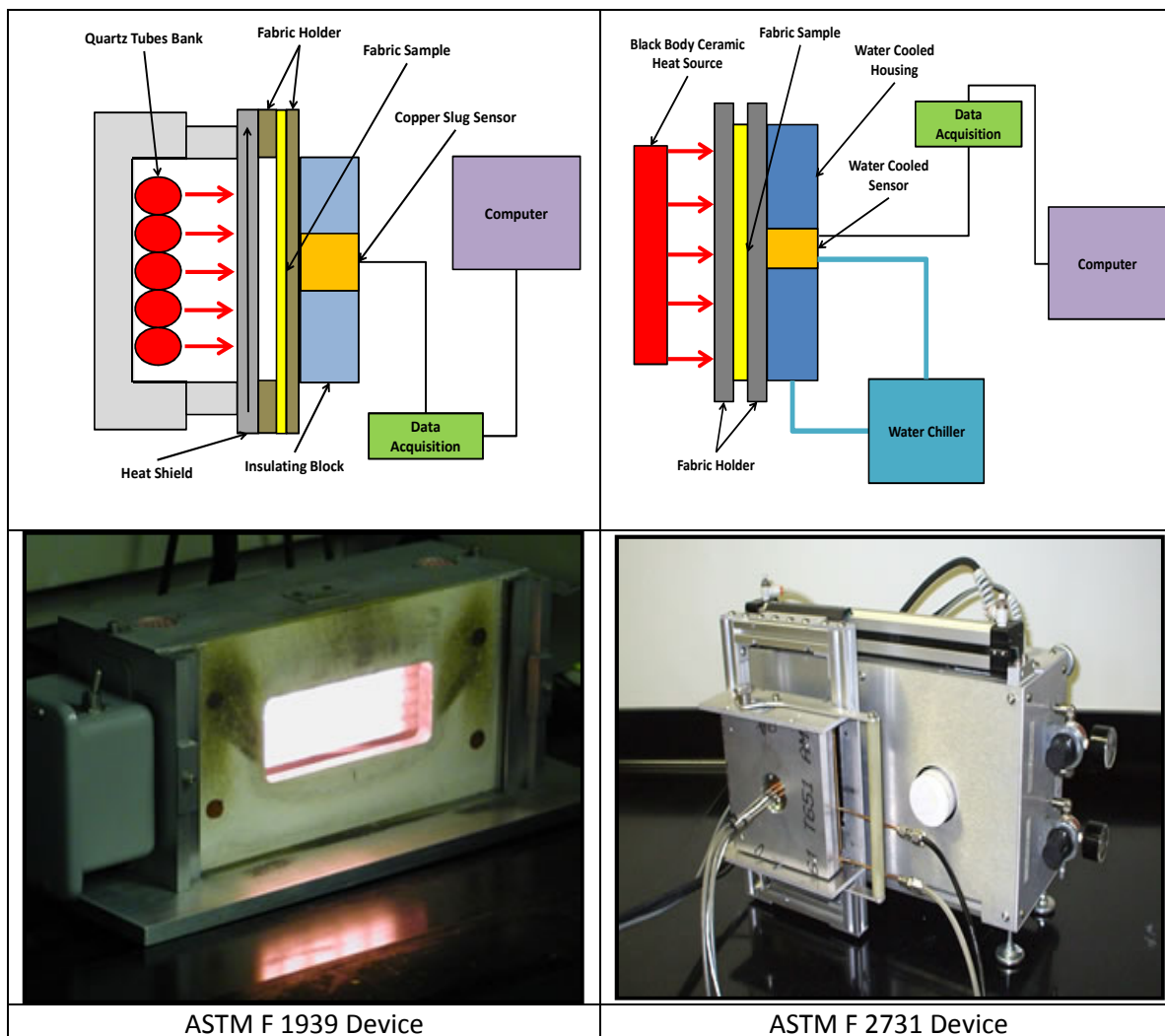


Figure 2-2: ASTM F 1939 (Left) & ASTM F 2731 (Right) Concept & Photographic Comparison

2.1.2 Burn Prediction Model Comparisons

ASTM F 1939 burn injury prediction method is calculated by comparing the input heat flux to the historic Stoll Curve [20] to determine time to second degree burn. Dr. Alice Stoll and her team conducted a series of experiments [20, 24] where subjects' forearms were

exposed to predetermined levels of thermal irradiance of less than 21 kW m^{-2} ($0.5 \text{ cal cm}^{-2} \text{ sec}^{-1}$). The volunteers were exposed to the heat flux until they received a “threshold blister,” where blister formation represents the presence of dermal damage, indicating a second degree burn. This data was later extrapolated for higher heat fluxes and compiled into a logarithmic shaped curve based upon the relationship between the known thermal properties of both human skin and the copper sensor used in RPP [20]. The original criteria had an upper limit of approximately 30 seconds. This extrapolation to lower fluxes with longer exposures could create issues with the prediction response due to the elongated test durations.

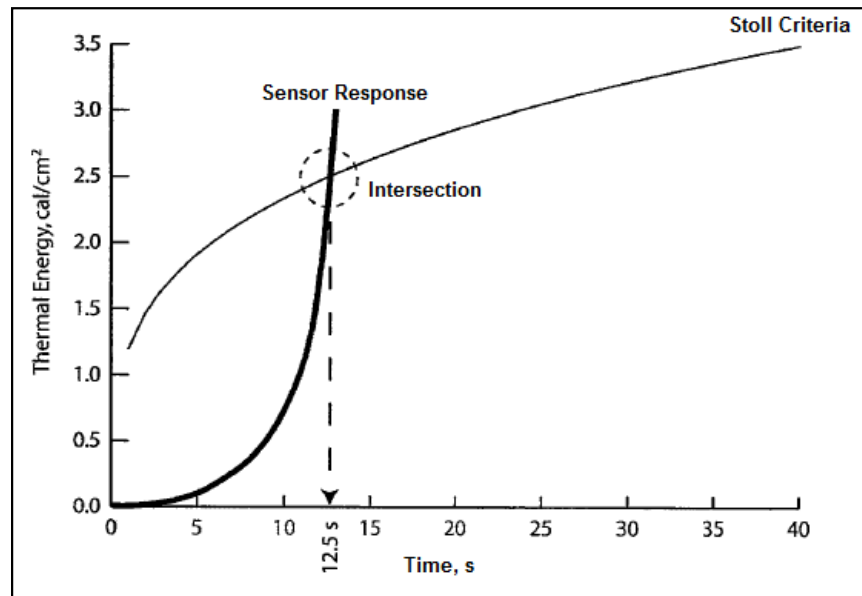


Figure 2-3: Stoll Curve demonstrating intersection point from sensor heat flux

Input heat flux from the copper calorimeter sensor is applied to the Stoll Curve and the time to second degree burn is found when the two curves intersect (Figure 2-3). This time to burn injury is multiplied by the applied heat flux to find the “RPP Value” (Equation 2-1), which is the index for protective performance of a fabric system.

$$RPP \left(\frac{\text{cal}}{\text{cm}^2} \right) = \text{Time to 2nd Degree Burn (seconds)} \times \text{Applied Heat Flux} \left(\frac{\text{cal}}{\text{cm}^2\text{s}} \right)$$

Equation 2-1: RPP Value

The ASTM F 2731 test device features improved burn injury predictions by using a human skin burn model that is more anatomically accurate for varying heat fluxes than the traditional Stoll Curve intersection method. This human skin burn injury model is based on (and validated by) the Stoll experiments [20, 24], but uses an anatomical model of human skin with burn injury criteria developed by Henriques [25]. This burn injury method is currently being used by fire test manikins (ASTM F 1930 [26]) and the Stored Energy Test (ASTM F 2731 [22]). ASTM F 2731 uses a burn injury prediction model that breaks the human skin into three layers, the epidermis, dermis, and subcutaneous (Figure 2-4). Each layer of skin has distinct properties for thickness (x), thermal conductivity (k), and volumetric heat capacity (ρC_p) as defined by ASTM F 1930 [26]. Heat flux measured from the water cooled sensor is applied to the surface of the skin and transferred through the skin using one-dimensional heat conduction (Equation 2-2).

$$k \frac{\partial^2 T}{\partial x^2} = \rho C_p \frac{\partial T}{\partial t}$$

Equation 2-2: One-Dimensional Conduction Equation

Where

- k = Thermal conductivity ($\text{W m}^{-1} \text{K}^{-1}$)
- T = Temperature (K)
- x = Depth into the skin (m)
- ρC_p = Volumetric heat capacity ($\text{J m}^{-3} \text{K}^{-1}$)
- t = time

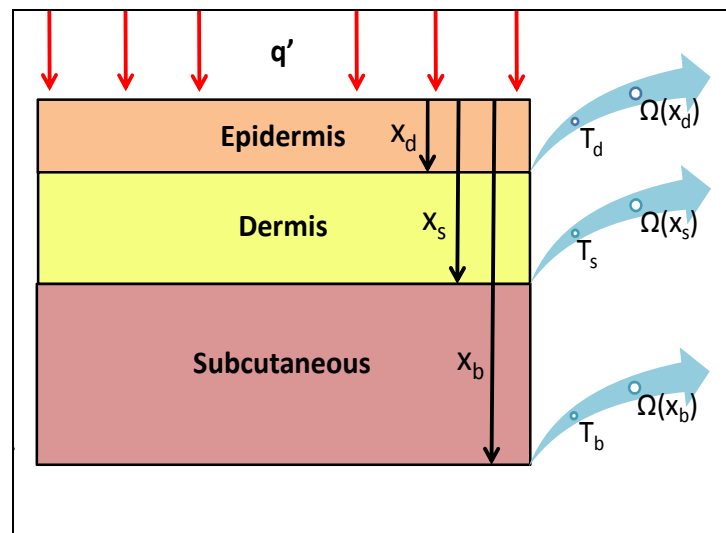


Figure 2-4: 1-D Burn Injury Prediction Model used in ASTM F 2731

The conduction equation provides temporal temperature for each of the layers of skin and burn injury is found by calculating Henriques Equation (Equation 2-3) at the epidermis/dermis junction. The pre-exponential (P) and activation energy (ΔE) constants are defined by ASTM F 1930 [26] and were derived from experiments by Weaver and Stoll [24].

$$\Omega = Pte^{-\Delta E/R(T+273)}$$

Equation 2-3: Henriques' Equation

Where	Ω	= Burn injury parameter
	P	= Pre-exponential constant (1 s^{-1})
	ΔE	= Activation energy constant (J kmol^{-1})
	R	= Universal gas constant ($8314.5 \text{ J kmol}^{-1} \text{ K}^{-1}$)
	T	= Temperature of skin (C)
	t	= Time temperature of skin above 317.15 K (seconds)

When solving Henriques Equation at the epidermis/dermis junction, $\Omega \geq 1$ results in a second degree burn injury, similar to the “threshold blister” value from the Stoll Curve. The values from the Stoll Curve are used as a bare exposure calibration to validate the human skin burn model, so replicating each of the data points from the Stoll experiments results in $\Omega \approx 1$. The advantage to using this model is that it more accurately represents human skin response and can compensate for a wider range of exposures, while still being validated by the Stoll Curve

for square-wave, bare skin exposures. The Henriques model also supplies additional information such as time to pain, 1st degree burn, 3rd degree burn, and total heat flux throughout the exposure.

Table 2-2: Comparison of Apparatus Properties

Properties of Platform	ASTM F 1939	ASTM F 2731
Heat Source	Quartz tube bank	Ceramic black body simulator
Intensity	21 kW m ⁻²	7.1 kW m ⁻²
Thermal Sensor	Copper slug calorimeter	Schmidt-Boelter thermopile
Burn Model	Stoll curve	Henriques

2.2 Experimental Procedures

This study compares ASTM F 1939 and F 2731 for use in evaluating heat resistant materials used in wildlands firefighter protective clothing ensembles. Table 2-3 describes the group of selected woven meta-aramid fabrics studied by this research. Standard testing protocol (found in the following sections) will be used by the two test methods. All of the samples were conditioned in a standard atmosphere for at least 24 hours prior to testing. A range of 93% meta-aramid, 5% para-aramid, and 2% antistatic fabrics were selected because this material is currently the standard outer shell fabric used by wildlands firefighter garments. Fabric layups were tested to resemble layered ensembles found in wildland

firefighter protective clothing including double layer samples and ensembles consisting of single layer fabrics over a knit base layer. 6.0 oz yd⁻² 100% cotton knit material used in CAL FIRE garments was incorporated into same fabric test ensembles.

Table 2-3: Materials

ID	Construction	Weight (oz yd ⁻²)	Thickness (mm)
Single Outer Shell System			
B	4.5 oz Plain	4.73	0.48
C	6.0 oz Plain	6.49	0.54
D	7.5 oz Plain	8.07	0.60
N	7.7 oz Twill	7.90	0.71
E	9.5 oz Plain	10.29	0.70
Double Outer Shell System			
BD	4.5 oz Plain / 7.5 oz Plain	12.87	0.99
Single Outer Shell with Base Layer System			
CI	6.0 oz Plain / 6.0 oz Knit 100% Cotton	13.48	1.10

2.3 Test Procedure Comparison

Fabric samples are cut to 4"x10" and then conditioned to 21°C and 65% relative humidity (RH) for at least 24 hours prior to testing in accordance with ASTM F 1939 [11].

Calibration for the RPP is performed by exposing the bare sensor to the radiant heaters for 10

seconds to ensure that the average heat flux over that time is $21 \text{ kW m}^{-2} \pm 2.1$. This calibration method is repeated after five fabric sample tests have been run to ensure that the test apparatus is producing constant heat flux over the duration of testing. Once calibrated, the fabric samples are tested within five minutes of being removed from the conditioned environment. Before each test, the sensor must be allowed to return to approximately $29 \text{ }^{\circ}\text{C}$ to maintain a constant starting point between experiments. Each specimen is placed within the fabric holder and exposed to the calibrated 21 kW m^{-2} until a 2nd degree burn occurs, where the time to 2nd degree burn is determined by the Stoll Curve [20].

The preconditioning protocol for the ASTM F 2731 device is the same as ASTM F 1939 (24 hours in 21°C and 65% RH). ASTM F 2731 fabric samples are cut to 6" x 6" squares. Calibration is performed by exposing the bare sensor to the heat supplied from the ceramic black body simulator for 70 seconds with the resulting flux averaged over the final 60 second time period. The calibration for ASTM F 2731 is significantly longer than for ASTM F 1939 to ensure that the applied heat flux is consistent throughout the longer duration exposures needed for lower intensity heat testing. ASTM F 1939 calibration can only be performed for 10 seconds due to heat saturation in the sensor and a maximum temperature cutoff of $100 \text{ }^{\circ}\text{C}$ from the copper calorimeter sensor.

Fabric samples for ASTM F 2731 are tested within five minutes of being removed from the conditioned environment. Every experiment begins with the sensor at an initial temperature of 32.5°C , which is the temperature of the water flowing through the sensor assembly and replicates human skin surface temperature. Each specimen is placed within the

fabric holder and exposed to the calibrated 7.1 kW m^{-2} until a second degree burn occurs. The time to second degree burn is determined by the human skin burn injury model using Henriques' burn injury parameter [25].

2.4 Results and Discussion

2.4.1 Effect of Test Method in RPP Ratings

Five replicate samples were tested using ASTM F 1939 and ASTM F 2731. The same samples preconditioning procedure was used for each method consisting of one washing as specified by NFPA 1977 [14] and AATCC 135 [27]. Figure 2-5 compares the RPP values obtained using these two different test methods. The error bars represent the observed standard deviation.

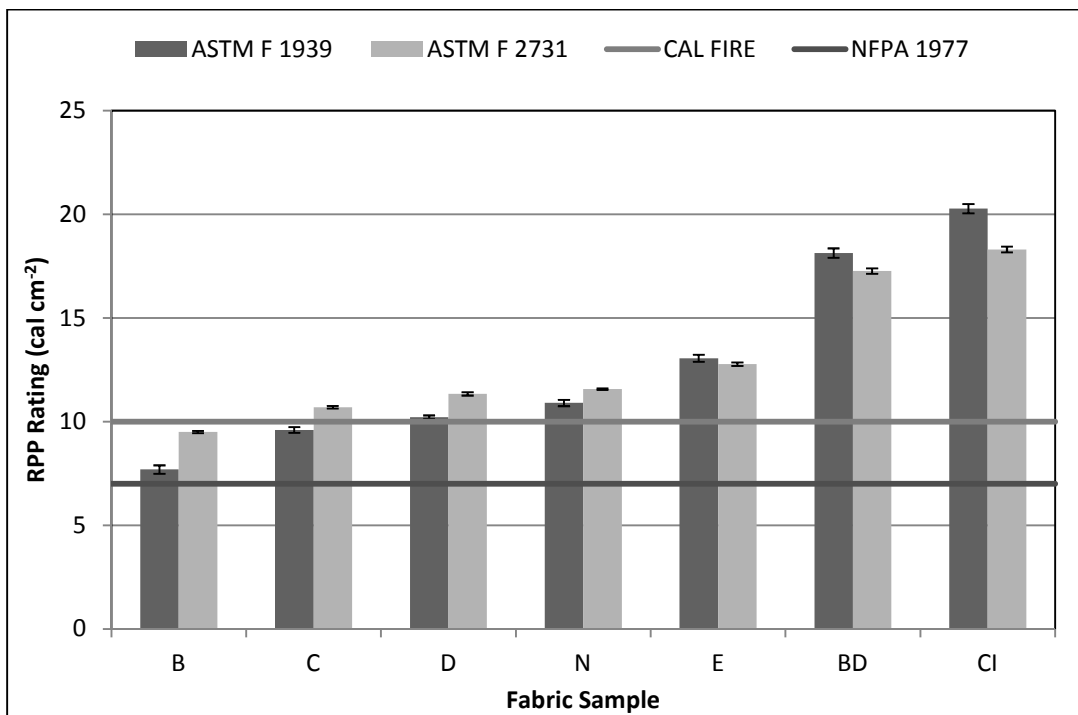


Figure 2-5: RPP Rating Comparison

Table 2-4: t Test Comparison of Significant Difference between Test Methods

	B	C	D	N	E	BD	CI
Significance Level	*	*	*	*	**	*	*

* = Significant difference at 95% level

** = Non significant difference at 95% level

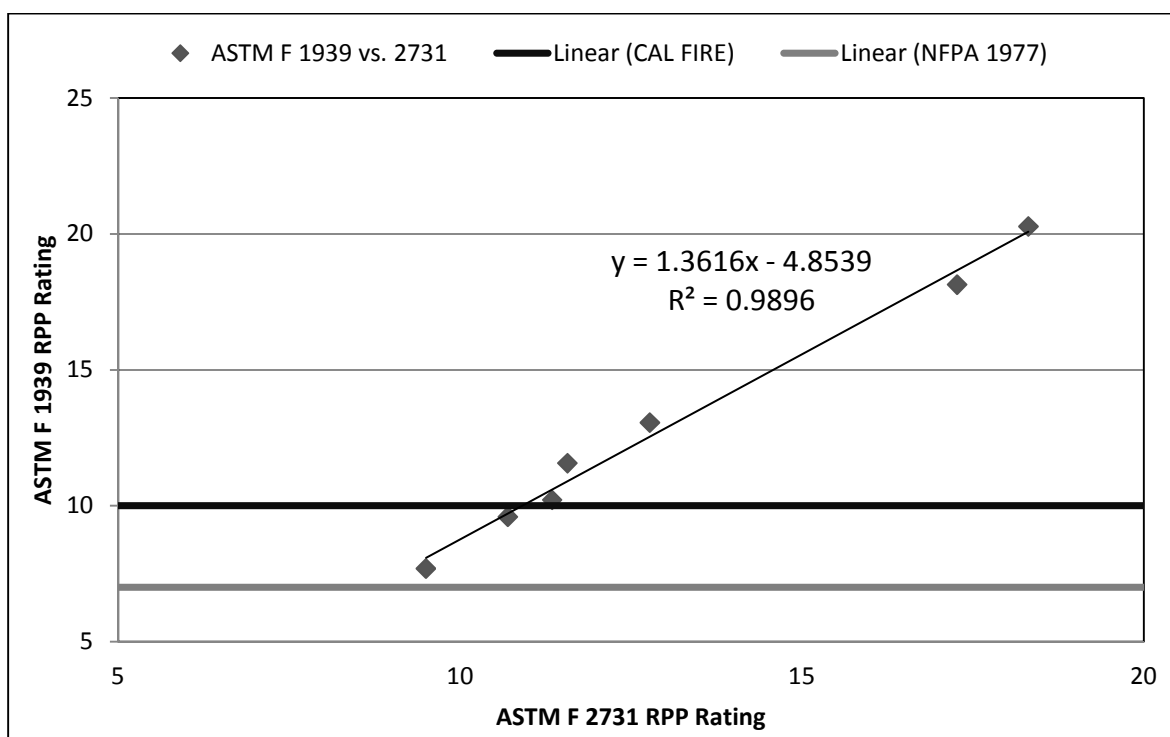


Figure 2-6: ASTM F 1939 vs. 2731 Correlation

Analysis of Figure 2-5 establishes that both test methods demonstrate an increase in protection as weight of fabric increases. It also shows that ASTM F 2731 consistently produces RPP values higher than ASTM F 1939 except for the heavier weight and double layer fabrics. This turning point occurs between fabrics N and E. It can also be seen that the inclusion of a second layer, whether it be a base layer or additional meta-aramid fabric, drastically increases the protection rating. Table 2-4 demonstrates that there is a significant difference between each test methods' RPP ratings with the exception of fabric E. Figure 2-6 establishes a very high correlation between both test methods.

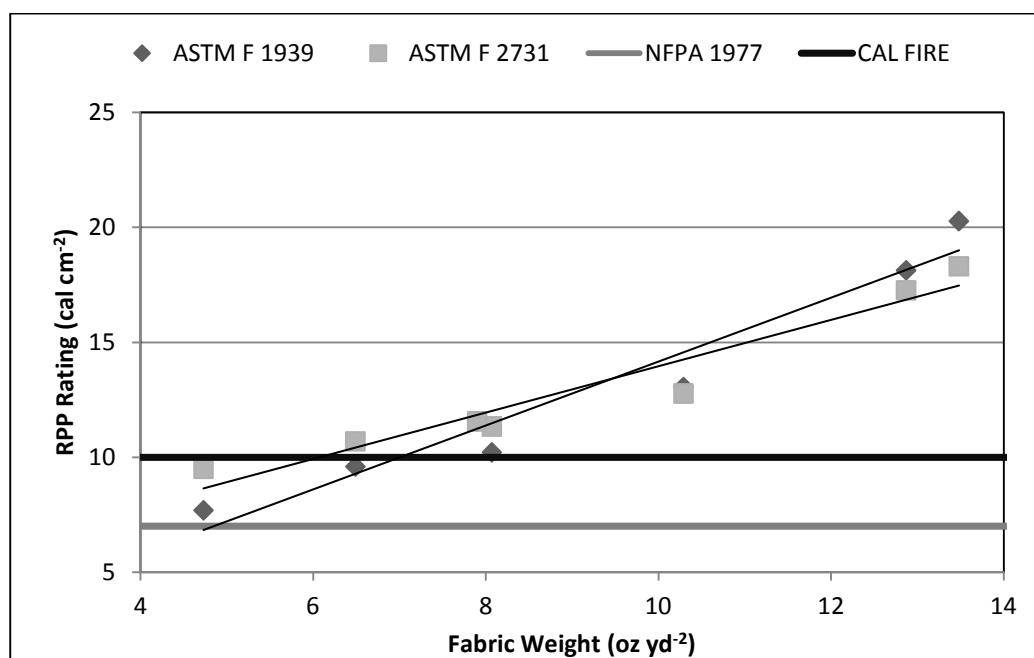


Figure 2-7: RPP Rating vs. Fabric Weight Test Method Comparison

Figure 2-7 demonstrates that in regards to the single layer configurations that the NFPA 1977 standard currently requires, the ASTM F 2731 platform delivers higher RPP values for fabrics up to 9.5 oz yd⁻² than its counterpart which could potentially permit lighter weight fabrics and ensembles which are more comfortable thus lowering heat stress cases.

2.4.2 Effect of Heat Exposure Intensity

The reduction of heat exposure intensity is the largest factor in the differences between the two test platforms as shown in Figure 2-8.

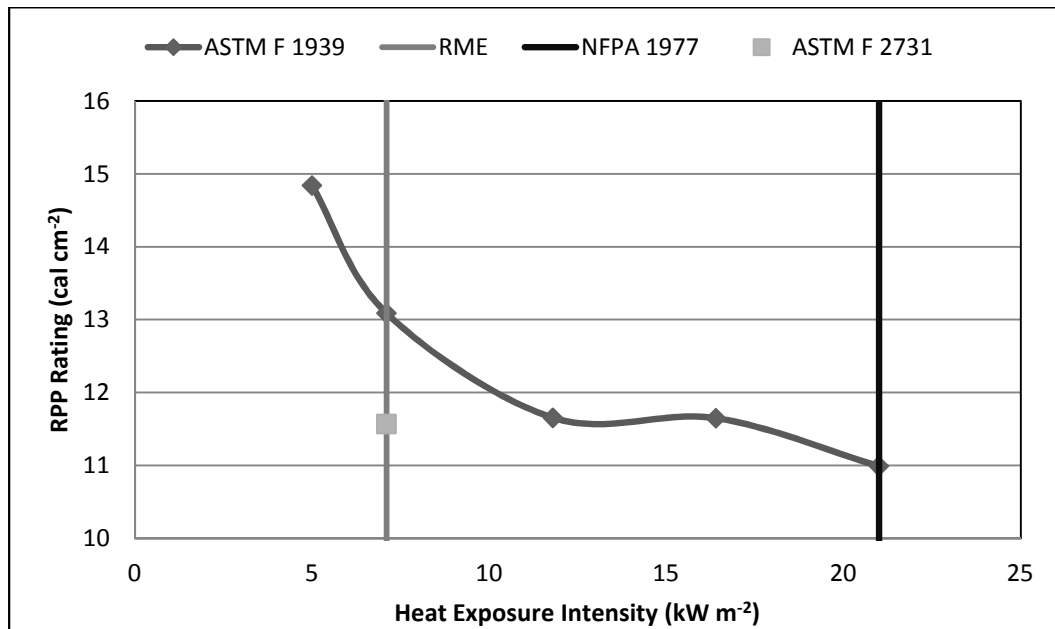


Figure 2-8: Effect of Heat Exposure Intensity in ASTM F 1939 on RPP for Fabric N

Figure 2-8 demonstrates a steady decline in protection predicted by the ASTM F 1939 apparatus as the exposure intensity increases. This is both a result of heat saturation in the lower exposures and fabric degradation in the higher exposures. A direct comparison at all five fluxes between both test methods is impossible as the ASTM F 2731 platform is unable to achieve fluxes above 10 kW m⁻².

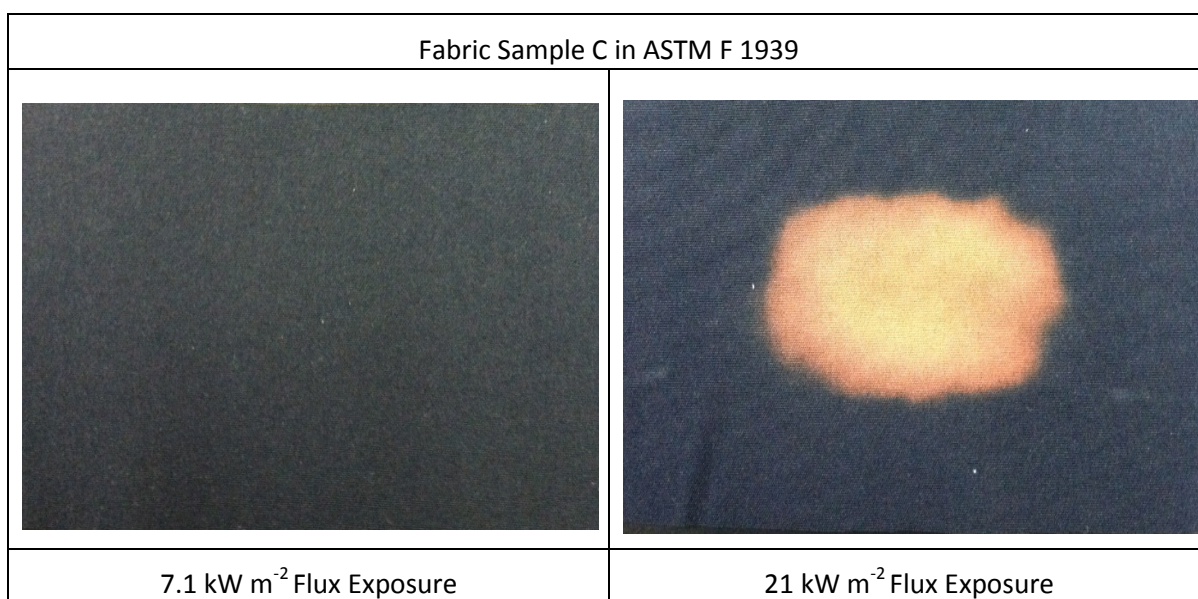


Figure 2-9: Exposure Intensity Degradation Comparison

The differences between degradation of fabrics between 7.1 kW m⁻² and 21 kW m⁻² are rather drastic. At RME intensity, the fabric experiences virtually no decomposition, while at the standard 21 kW m⁻², the fabric becomes brittle and the majority of the dye burns off at the point of exposure. The degradation witnessed at the higher intensity can potentially skew results obtained utilizing the ASTM F 1939 test methodology. This is due to the fiber shrinkage that occurs at this exposure point which causes breakthrough where additional heat can flow through unimpeded.

2.4.3 Effect of Test Platform Differences

A key aspect of this study was to establish that ASTM F 1939 does not perform efficiently at RME intensity as a result of heat saturation present in the copper calorimeter sensor which can be corrected with the use of water cooling found in ASTM F 2731.

Evaluating the heat saturation differences between the water cooled sensor and standard copper slug sensor was performed by taking the instantaneous heat flux traces over time from single layer meta-aramid fabric testing. Typically, RPP tests conclude immediately after a second degree burn injury occurred; however in this study, the test was continued for additional time to more clearly demonstrate the declining heat flux trend before second degree burn is achieved. Each curve is the result of an average of three repetitions

To determine if there are differences between test methods that is not a product of sensor type, the water-cooled sensor from ASTM F 2731 was tested in the ASTM F 1939 apparatus and compared to the original response (Figure 2-10) and vice versa (Figure 2-11).

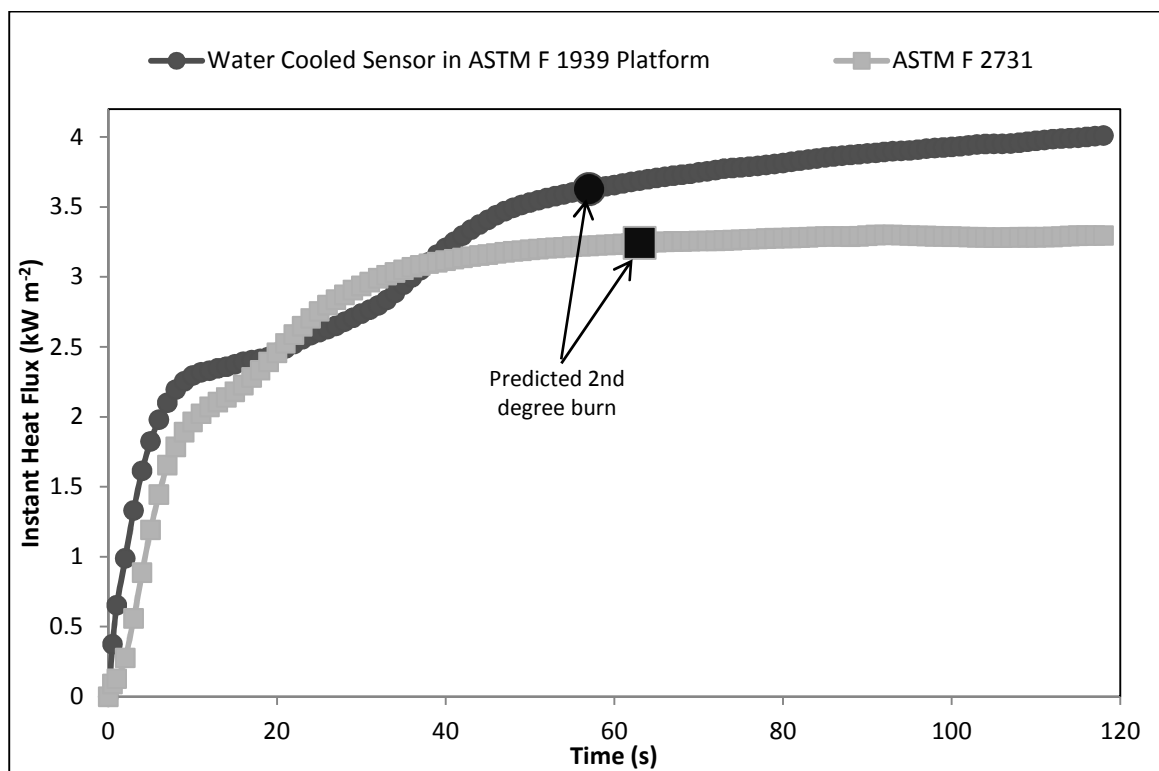


Figure 2-10: Instant Heat Flux Comparison between Water Cooled Sensor in Both Test Platforms at RME Exposure Intensity for Fabric C

The trends in both curves of Figure 2-10 are very similar until 40 seconds into the test where the trace keeps increasing in the ASTM F 1939 platform. The ASTM F 2731 trace remains steady and does not keep rising. This is a result of the automatic feed-back system present in ASTM F 2731. The apparatus automatically detects the flux being emitted and adjusts itself accordingly to maintain constant flux levels. The ASTM F 1939 apparatus does not possess this feature and instead supplies a constant amount of power to the heat source even though the flux may keep increasing as a result.

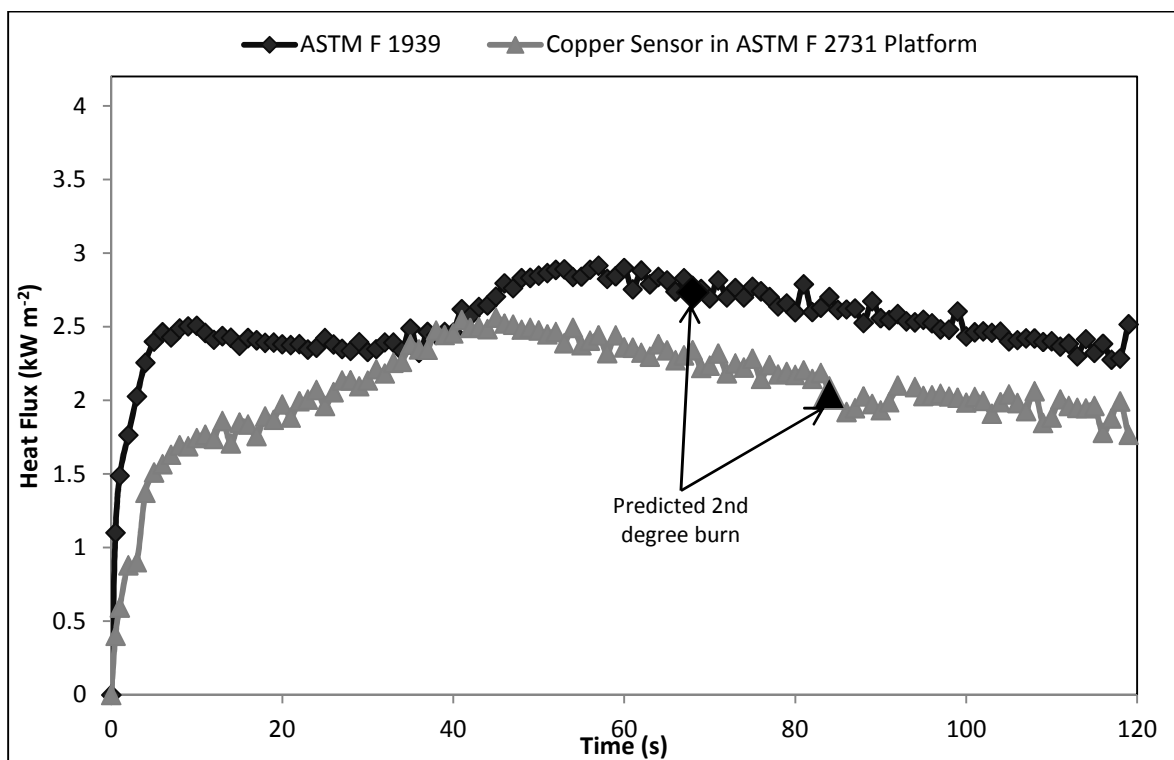


Figure 2-11: Instant Heat Flux Comparison between Copper Sensor in Both Test Platforms at RME Exposure Intensity for Fabric C

Figure 2-11 is a comparison between two instant heat flux traces; one that represents the standard ASTM F 1939 test platform and the second which represents the copper slug sensor and ceramic insulation block implanted into the ASTM F 2731 test platform. This was done to isolate whether differences in the curves are a result of the sensor or some variation from the apparatus. The primary feature to take away from Figure 2-11 is that the curves from two different heating elements are significantly different from one another even with the same sensor and data acquisition unit. Prominent features from the ASTM F 1939

curve include the sharp initial rise from the beginning of the test, followed by a slight reduction in detected flux, which will be referred to as the “dip”, and then a second increase followed by another reduction which can be attributed to the heat saturation of the copper sensor. It is important to note that these specific trends are not displayed in the water cooled sensors in Figure 2-10.

Due to the fact that the dip is only present in the ASTM F 1939 curve and not the other, even though they possess the same sensor, the conclusion can be made that it is a product of some element of the test apparatus other than the sensor. It is possible that the dip is a function of the fabric specimen size as compared to the heat exposure view factor. The ASTM F 1939 fabric sample is 4” x 10”, where only a 2.5” x 6” window is exposed to the thermal energy. This leaves a 1.5” gap on the top and bottom of the sample and a 4” gap on the sides (25 in² blocked from heat by specimen holder) where heat can conduct laterally away from the main exposure area to the cooler fabric. Conversely, the fabric sample of the ASTM F 2731 platform, which was used for the other curve, possesses a 6” x 6” area, where the space being exposed to the heat is 5” x 5”. This leaves only a 1” gap on all sides (11 in² blocked from heat by specimen holder) for heat to conduct laterally through the fabric. Therefore the dip seen in the ASTM F 1939 apparatus is a result of heat laterally conducting from the viewing area to the cooler areas behind the sample holders. This dip becomes more pronounced for heavier weight fabric as seen in Figure 2-12.

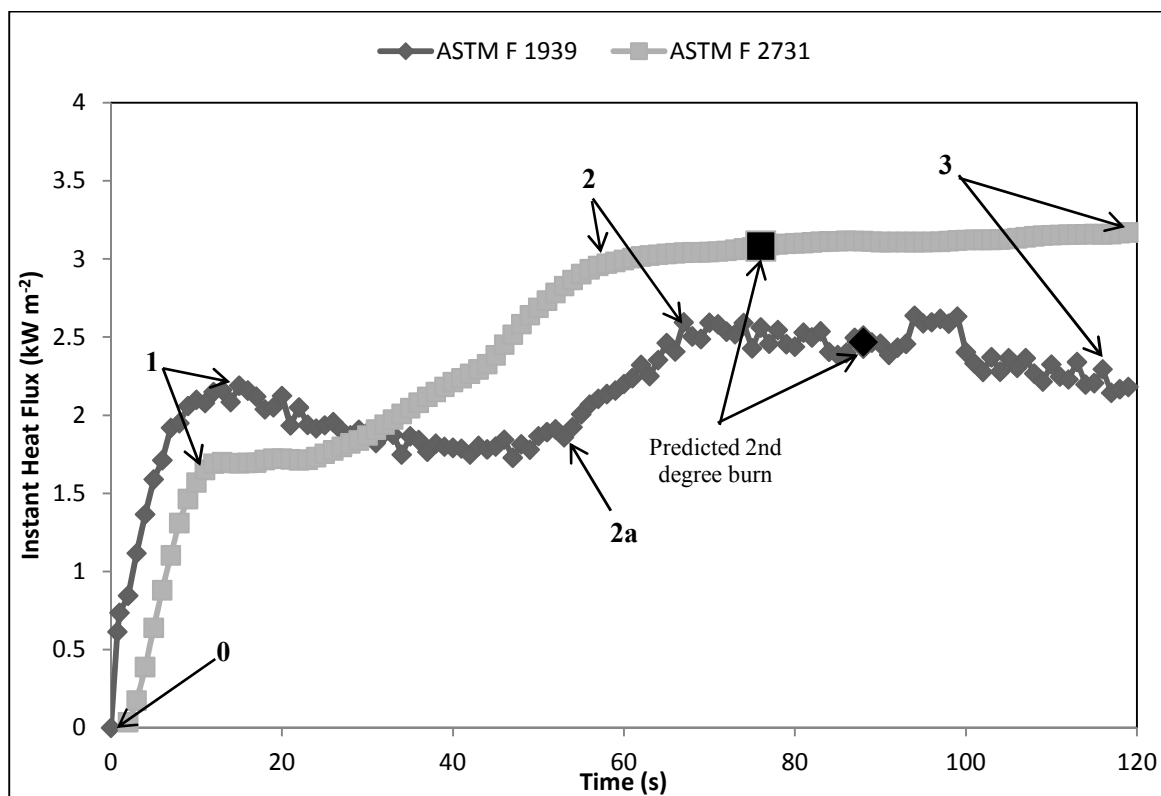


Figure 2-12: ASTM F 1939 vs. ASTM F 2731 Instant Heat Flux Comparison at RME Exposure Intensity for Fabric E

Figure 2-12 represents a comparison of instant heat flux traces between the two main test platforms investigated in this study; ASTM F 1939 and ASTM F 2731. It can be seen that from points 0 to 1, for Figure 2-12, both curves initially rise quickly and peak, demonstrating the heat passing through the fabric to the sensor (not conducting into the fabric sample). The slopes for the two lines are nearly identical; however, there is a slight offset between the two lines due to the data sampling differences in the two devices. From points 1-2, both sensors show the fabric absorbing radiant heat flux; heating up to a temperature,

and re-radiating heat to the sensor. From 1-2a for the copper sensor in the ASTM F 1939 platform, the dip represents the fabric sample conducting heat to other portions of the fabric sample and sample holder. However, in theory, the detected flux should not fall below the initial peak at point 1 as this is the amount of flux the fabric lets pass through. This can be explained by the fact that the fabric surface is still being heated causing the fibers to expand and reflecting a portion of the incident heat passing through the fabric. This is not as prevalent on the water cooled sensor of ASTM F 2731 because the fabric is heating at a faster rate due to the larger exposure region and significantly less unexposed area behind the fabric holder. From 2a-2, the fabric sample reaches a sufficient temperature to re-radiate additional heat to the sensor and begins to increase the detected flux. From 2-3, heat saturation in the copper sensor takes place which is not present in the water cooled sensor.

2.4.4 Effect of Burn Model

Both ASTM F 1939 and ASTM F 2731 utilize different burn injury models; Stoll and Henriques respectively. The same flux curve for ASTM F 1939 at RME exposure intensity which used the Stoll criteria to calculate the second degree burn time was put into the Henriques model to determine if burn model had a significant effect on the results.

Table 2-5: Burn Model Prediction Comparison

Sample	Stoll Time to 2 nd Degree Burn (s)	Henriques Time to 2 nd Degree Burn (s)
C	67.60	67.32
N	77.40	75.55
E	89.56	89.01

Both models returned very similar results proving that the key differences between these two test methodologies are the platforms themselves and not the burn models. However, we still advocate the use of Henriques over Stoll as the former supplies more information such as time to pain, 1st degree burn, 3rd degree burn, and total heat flux throughout the exposure.

2.4.3 Repeatability Validation of Both Test Methods

Testing was performed to establish intra-laboratory precision on three meta-aramid samples (B, N, E) of varying weight and construction. The test plan was constructed in accordance to the precision and repeatability protocol in ASTM E 177 *Standard Practice for Use of the Terms Precision and Bias in ASTM Test Methods* [28]. All experiments were conducted by a single operator over the shortest time period possible to ensure the lowest variability. Tests were carried out to acquire the time to 2nd degree burn as estimated by the respective burn injury model. All data was analyzed using the statistical methods recommended by ASTM E 177 to assess the precision and repeatability of measurements.

Table 2-6: Repeatability Study for ASTM F 1939 & ASTM F 2731

ASTM F 1939						
	B		N		E	
Set Tested	Average (s) ¹	Std Dev	Average (s) ¹	Std Dev	Average (s) ¹	Std Dev
1	15.82	0.39	23.71	0.49	26.57	0.64
2	15.95	0.50	23.69	0.53	27.54	0.77
3	15.39	0.82	23.33	0.26	27.14	0.71
Grand Average ²	15.72		23.57		27.08	
Grand Std Dev	0.566		0.425		0.705	
Grand %CV	3.6		1.8		2.6	

Table 2-6 Continued						
ASTM F 2731						
	B		N		E	
Set Tested	Average (s)	Std Dev	Average (s)	Std Dev	Average (s)	Std Dev
1	57.44	0.65	71.04	0.78	76.31	0.60
2	57.72	0.79	70.83	1.25	77.72	0.64
3	57.81	1.21	70.08	1.38	76.45	0.48
Grand Average	57.66		70.65		76.83	
Grand Std Dev	0.881		1.136		0.572	
Grand %CV	1.53		1.61		0.74	

¹ Average of 5 replicates tested each day.

² Average of 15 of replicate measurements

The data in Table 2-6 establish that the ASTM F 2731 apparatus provides results just as consistent or more with minimal variability when performed within the same laboratory and conducted by a single operator when compared to results obtained from ASTM F 1939. The coefficient of variations in ASTM F 2731 for all fifteen replicates never exceeds 1.61% and the standard deviations of a single set of five replicates never exceed 0.82. Results with such low variability will be necessary for acceptance as a standardized test procedure. The extremely low standard deviations of the ASTM F 2731 platform are a direct result of the majority of automated functions not otherwise found in ASTM F 1939.

2.4.4 Material Discrimination Experiments

A necessary aspect of this research was to prove that the ASTM F 2731 device is capable of responding to known differences in weight and construction of fabric samples. The single layer fabric configurations from Table 2-3 were tested for 5 replicates using the respective test platform and results of experiments are shown in Table 2-7.

Table 2-7: Differentiation of Both Test Platforms

Sample	ASTM F 1939		ASTM F 2731	
	Average Time to 2nd Degree Burn ¹	Std Dev	Average Time to 2nd Degree Burn ¹	Std Dev
B	15.4	0.82	55.9	0.67
C	19.2	0.56	62.9	0.69
D	20.4	0.35	66.7	0.93
N	21.8	0.61	68.1	0.48
E	26.1	0.71	75.2	0.90

¹ Average of 5 replicates

The data in Table 2-7 shows that results from both test methods are affected by differences in the construction and weight, as weight increases, estimated time to second degree burn also increases. The actual weights of each fabric reported in Table 2-3 show that sample N is actually lighter weight than sample D. However, the twill weave present in specimen N creates makes the fabric thicker and gives a higher time to burn than specimen D. Results from ASTM F 2731 supplied more consistent values with lower standard deviations.

T-tests were carried out to establish if there were any significant differences between sample weights. The T-test compares sample sizes, variances, and the means of two separate groups of data and returns a p-value which specifies the probability that the data is a result of chance. A p-value of less than 0.05 is significant at a 95% interval and a p-value of 0.01 is significant at a 99% interval. The tests showed that the measured time to 2nd degree burn for all fabric samples are statistically different from one another with at least a 99% level of

statistical significance, with the exception of the comparison made between D and N with the ASTM F 2731 platform which fell in the 95% range. With fabrics so close together in weight, ASTM F 2731 was still able to differentiate between the two very well with a high level of statistical difference. These tests can be found in Appendix A.2.

2.5 Conclusions

Research into the current standard ASTM F 1939 test method demonstrated a number of limitations in the test apparatus when applying a lower incident heat flux, which would be applicable for wildland firefighter protective clothing testing. The limitations of the ASTM F 1939 (heat saturation, burn injury prediction, human error, etc.) are all improved upon by the ASTM F 2731 device. ASTM F 2731 has been shown to provide an enhanced evaluation of wildland firefighter thermal protective clothing. It utilizes an automated shutter system, water cooled sensor, steadier heating source, and an improved human burn injury prediction model which produces a more accurate test method for low intensity heat flux testing. The ASTM F 2731 platform and test method was also shown to be a very repeatable test method as well as differentiate between fabrics of different weights, even when the weights are very similar. Throughout this study, it was shown that the key factor that influences RPP rating is the heat exposure intensity; a reduction in exposure intensity will improve the predicted time to second degree burn. This reduction in exposure flux that the ASTM F 2731 platform is able to accommodate, could potentially allow for lighter weight fabrics in wildland firefighter protective clothing which would allow for improved total heat loss values (THL) and overall comfort [29]. This study focused primarily on meta-aramid fiber responses to

heat but it stands to reason that fibers with higher thermal stability such as polybenzimidazole (PBI) could possibly mitigate the difference between 7.1 and 21 kW m⁻² exposure flux RPP ratings due to the lower decomposition in higher fluxes.

CHAPTER 3: EVALUATION OF WILDLAND FIREFIGHTING MATERIALS

3.1 Introduction

Wildlands firefighters encounter thermal dangers that are typically not observed by structural firefighters. Wildlands firefighters routinely operate in a variety of weather conditions that range from 63-91 °F and 14-81 %RH [15]. Except for extreme scenarios, they typically fight fire from a distance and only need to be protected from low to moderate levels of radiant heat. During a Risk Assessment Study, California Department of Forestry and Fire Protection (CAL FIRE) [7] characterized a “reasonable maximum exposure” (RME) level of 7.1 kW m⁻² (0.17 cal cm⁻² sec⁻¹) and is defined as “the upper range of ordinary work conditions”.

The Radiant Protective Performance (RPP) test method (ASTM F 1939) [11] for measuring the heat resistance of personal protective equipment (PPE), was originally established to simulate heat flux intensities specific to structural firefighters, testing for heat fluxes of 84 kW m⁻² (2.0 cal cm⁻² sec⁻¹). Later revisions of the test method were adopted for wildlands protection by reducing the heat flux exposure to a more “practical” level of 21 kW m⁻² (0.5 cal cm⁻² sec⁻¹). However, the CAL FIRE risk assessment has demonstrated that even

this reduced level of 21 kW m^{-2} ($0.5 \text{ cal cm}^{-2} \text{ sec}^{-1}$) is still a great deal higher than what is actually required to accurately represent realistic wildfire conditions, such as the RME value.

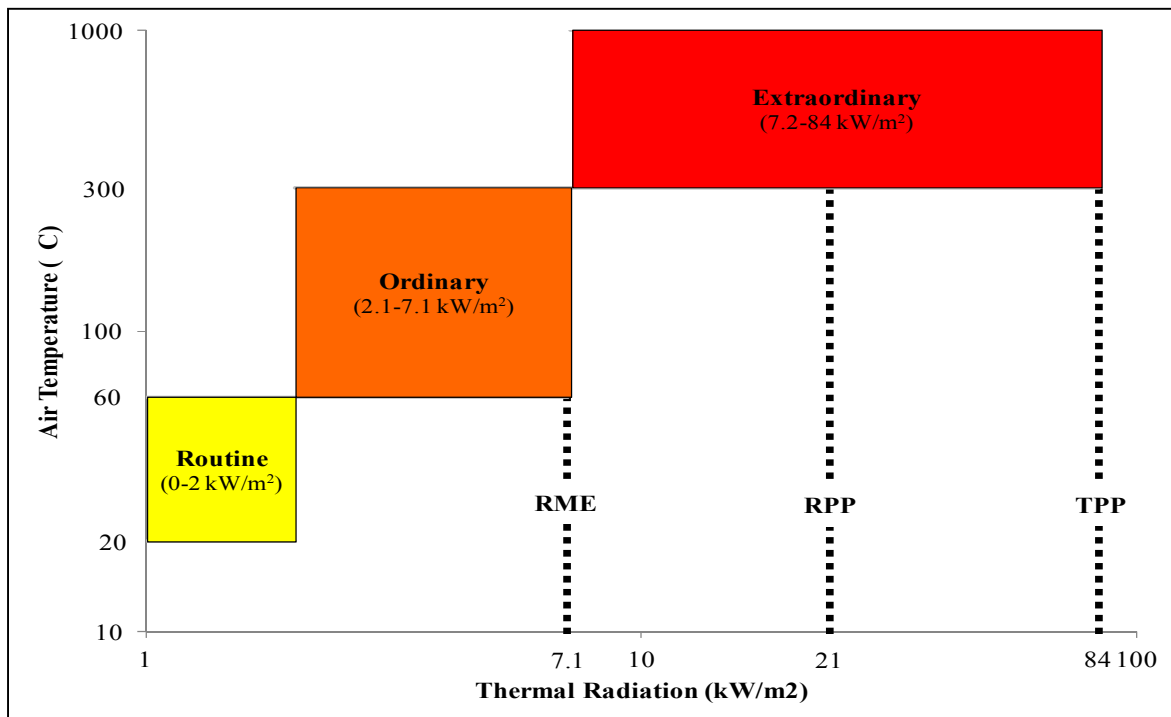


Figure 3- 1: Wildland Environment Thermal Ranges

According to the NFPA 1977 [14] standard, for a fabric to pass the thermal protection minimum it must achieve an RPP value of at least 7 cal cm^{-2} . CAL FIRE [7] has established an internal standard requirement of 10 cal cm^{-2} for their garments. This value is recommended in order to protect a firefighter for the 60 seconds, the maximum time it should take a firefighter to react to a dangerous situation by leaving the area or deploy a fire shelter

if needed. A fabric exposed to the standard 21 kW m^{-2} will attain a 2nd degree burn much faster than one at 7.1 kW m^{-2} and, by taking heat flux into account we are able to directly compare the protection gained by that textile. The premise behind the RPP test is to achieve a time to 2nd degree burn and thus an RPP value.

Ideally, lowering the RPP exposure heat flux will augment the protection provided by the wildlands firefighter fabric, this will open the door for lighter weight garment options that defend against thermal hazards as well as improve comfort for firefighters which is of the utmost importance. A collection of data from the years 1990-2006 shows that more wildland firefighters were killed from heart attacks than burn injuries [1]. The majority of these heart attacks are a direct result of the thermal strain imposed on the firefighters by their PPE. With this revelation in mind, a shift in priorities from protection to comfort in PPE is warranted. This study demonstrates a test method for evaluating the radiant protective performance of wildland garments for RME levels which will determine the effect of heat exposure intensity on RPP of FR fabrics and base layers used in PPE as well as compare the impact of testing at the required higher flux to the RME flux.

3.2 Reasonable Maximum Exposure

For the current RPP test method, the 21 kW m^{-2} incident flux represents an “extraordinary” exposure in which wildlands PPE would not be able to protect against for an extended period of time. The identification of an RME flux is the result of a number of studies performed on wildlands firefighting conditions [15], primarily the 2010 CAL FIRE risk assessment study [7], which described the Reasonable Maximum Exposure (RME)

intensity of 7.1 kW m^{-2} as the upper limit of the “ordinary” range of heat flux experienced by wildland firefighters. CAL FIRE arrived at this value by using the Cohen flame radiation model [8] found in Equation 1.

$$\dot{q}_w'' = F_{f,w} \varepsilon_f \sigma T_f^4$$

Equation 3- 1

Where \dot{q}_w'' = Incident heat flux (W m^{-2})

$F_{f,w}$ = View factor

ε_f = Emissivity

σ = Stephan Boltzmann constant ($\text{J m}^{-2} \text{ s}^{-1} \text{ K}^{-4}$)

T_f = Temperature (K)

The radiant heat flux incident (\dot{q}_w'') on a firefighter can be calculated when the parameters of the flame are known, particularly size (height, width, depth) and intensity (temperature).

View factor ($F_{f,w}$) can be estimated if the spatial relationship between the flame wall and firefighter is defined. This relationship is created by modeling a rectangular flame wall of known size dimensions and a flat surface representing a firefighter a set distance away (Figure 3- 2) [8].

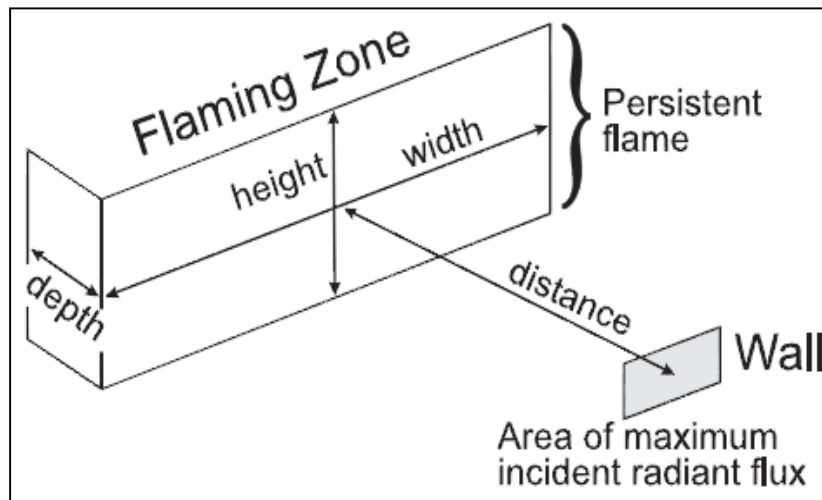


Figure 3- 2: Cohen Flame Radiation Model

CAL FIRE [7] defined the flame wall and distance parameters by referring to the Hauling Chart from the United States Forest Service (USFS) handbook [30]. The minimum safe operating distance from a fire is 1 foot away when there is a flame wall 100 meters wide, 3 meters deep, and 1 meter high. The depth of 3 meters for the flame wall, was chosen to make the fire “optically thick”, meaning that the heat source can be regarded as a black body with an emissivity (ϵ_f) of 1.0 [8]. 100 meters was chosen to assume an “infinite length,” which makes calculating the view factor ($F_{f,w}$) easier for Equation 3-1. The temperature of the flame wall is assumed to be 1200 K for these estimations.

Recent wildlands firefighting studies confirm CAL FIRE’s RME value. Australia’s Project Aquarius 4 [15] performed a series of controlled brush fires and 283 spot readings were recorded via a calibrated radiometer. Their data showed a range of fluxes from 0.5 to 8.6 kW m⁻² with the latter representing their “RME”. Packham and Pompe [18] established

the maximum flux and temperature from a brush fire to be 6.3 kW m^{-2} and 1200 K respectively by estimating the flame's view factor through pictures of forest fires and measured their intensity using radiometers. Phani K. Raj [16] carried out an experiment where controlled liquefied natural gas (LNG) fires were lit and the resulting flux was recorded depending upon the distance from the flame. The recorded flux range was between 3.5 to 5 kW m^{-2} with a few instances where the maximum reached approximately 7 kW m^{-2} . All of these studies [7, 8, 15, 16, 18] provide flame temperatures and fluxes that are within the same range as the defined RME value of 7.1 kW m^{-2} and well below the standard 21 kW m^{-2} currently being used by the RPP test method, providing justification for the use of an RME exposure flux for future RPP testing. Table 2-1 provides a summation of these studies.

3.3 Wildland Firefighter Garments

The garments worn by wildland firefighters possess a wide range of weights and thicknesses when accounting for every layer worn including base layers and overlapping clothing. Currently, the most commonly used garment configuration is regulated by the US Forest Service which utilizes a set of single layer pants and jacket. In contrast, the clothing regulated by CAL FIRE requires the use of a heavier set of double layer pants and single layer jacket. Research into systems similar to these will provide useful information in determining which fabric configuration is best. All PPE fabrics for wildlands firefighting must be certified by NFPA 1977 [14], however the standard does not consider the benefit that base layers provide for thermal protection. Consideration of how the standard issue cotton in both USFS and CAL Fire performs as well as moisture wicking knit fabrics like

thermoplastic polyesters and modacrylic blends is an important issue when discussing overall protection. Research has shown that thickness is a major contributor to thermal protection due to the additional air layering which suggests that inclusion of base layers will provide a sizable enhancement to protection. The research performed in Chapter 2 discussed the comparison of the standard ASTM F 1939 and the proposed ASTM F 2731 for the evaluation of thermal protection provided by PPE fabrics. The purpose of this study is to investigate the effects of fabric weight, layering and base layers on RPP measurements at the RME exposure intensity.

3.4 Experimental

The concept of a RME heat flux will be used in this study to determine its effects on fabric and base layers used in PPE when compared to the standard higher flux test results as well as how the ASTM F 2731 test platform responds to a RME flux.

3.4.1 Test Materials

Table 3- 1 describes the test materials studied by this research. Meta-aramid blends were selected for the outer shell because it is currently the standard material used in wildlands firefighter garments. Using more material types would have only served to add extra variables that would make direct comparisons difficult. The materials selected represent a range of weights and constructions that are similar to the garments currently used in the field. These materials also include both single and double layer systems comparable to what is found in wildlands firefighting clothing. It has been well documented that the controlling factor of thermal protection comes from weight and thickness, not fiber

composition. Four base layer materials were chosen to represent t-shirt and undergarment materials worn by wildland firefighters. Polyester is not recommended for use by firefighters in the field because it is a thermoplastic material that can melt at high temperatures. However, since it is a performance material and widely available, it is possible that firefighters wear it by accident and evaluating the fabric in this study is useful. Fabrics A through N are comprised of 93% meta-aramid, 5% para-aramid, and 2% antistatic fiber.

Table 3- 1: Test Materials

ID	Construction	Weight (oz yd ⁻²)	Thickness (mm)
A	Plain Weave	3.4	0.25
B	Plain Weave	4.7	0.48
C	Plain Weave	6.5	0.54
D	Plain Weave	8.1	0.60
E	Plain Weave	10.3	0.70
F	Twill Weave	5.7	0.55
G	Twill Weave	6.2	0.54
H	Twill Weave	7.3	0.55
N	Twill Weave	7.9	0.71
I	100% Cotton Jersey Knit	7.1	0.64
J	100% Cotton Jersey Knit	4.7	0.51
K	100% Polyester Jersey Knit	4.6	0.46
L	Modacrylic Blend 1x1 Warp Rib Knit	5.12	0.54

3.4.2 Methods

The experiments in this study were performed using the ASTM F 2731 test platform [22] which was originally developed for evaluating transmitted and stored thermal energy in longer duration radiant heat exposures by North Carolina State University and Measurement

Technologies Northwest [23]. The elements of the ASTM F 2731 test apparatus include a heat source, heat flux sensor, specimen holder, and data acquisition system. The device possesses a water cooled sensor block to simulate the temperature and blood flow effects of human skin and an automated shutter system to reduce human operator variation in the test platform. The sensor is a water cooled Schmidt-Boelter sensor, set to a human skin temperature of 32.5 °C. The heat source used is a ceramic black body simulator which provides a very consistent exposure flux that closely replicates the wave form of fires and utilizes control feedback that enables the system to maintain steadier flux outputs. The heat flux has been altered from the suggested 8.5 kW m⁻² in ASTM F 2731 to the 7.1 kW m⁻² RME flux. It has been demonstrated that ASTM F 2731 provides excellent reproducibility due to the automated functions such as transfer tray movement and controlled power feedback [23]. The compression and moisture conditioning aspect of ASTM F 2731 was not used for these experiments. Samples were conditioned in a standard atmosphere of 21 °C and 65 % relative humidity for at least 24 hours prior to exposure. Each data point represents the average of five replicates. The design of these experiments was to evaluate the protection provided by single layer fabrics of varying weights, multiple layer systems, as well as the effect of a range of base layers in conjunction with outer shell fabrics.

3.5 Results and Discussion

The first set of experiments in Figure 3- 3 conducted included an average of RPP values for every fabric configuration tested from materials in Table 3- 1, plotted against the NFPA 1977 [14] of 7 cal cm⁻² and CAL FIRE [7] of 10 cal cm⁻² standard to verify whether

the values passed the minimum criteria. CAL FIRE's rationale for their standard minimum stems from the PPE providing thermal protection for 60 seconds before a 2nd degree burn occurs. 60 seconds of protection using 7.1 kW m⁻² would provide a RPP value of 10. The error bars in all following graphs correspond to the data's representative standard deviation.

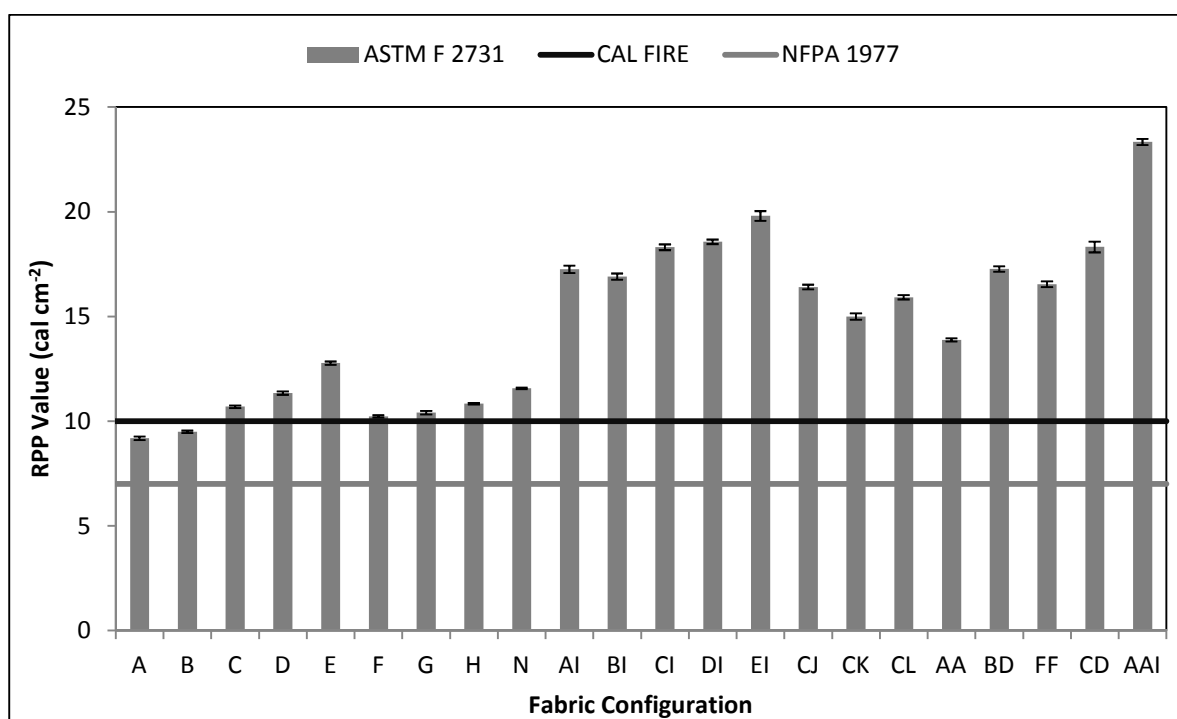


Figure 3- 3: RPP Ratings

Figure 3- 3 shows that as fabric weight increases, the protection value also increases. Differences between the twill woven fabrics are slightly more subtle than the plain woven constructions, primarily due to similarity in weight and thickness. Every fabric tested by the

ASTM F 2731 platform produced an RPP value that at least passed the NFPA 1977 criteria of 7, while the majority passed the more rigorous CAL FIRE minimum of 10. It is interesting to note that when the outer shell meta-aramid fabrics were tested with either a base layer or in a double layer system, it passed the criteria easily, sometimes doubling it. The air layers between fabrics also contribute a significant portion of the protection provided. Fabric configuration AA is approximately equal to sample C in weight however the former performs better by a good margin as a result of the air trapped between the two lightweight fabrics. Figure 3- 3 also demonstrates that even fabrics that are typically avoided such as thermoplastics like polyester provide an increase in protection as evidenced by configuration CK when compared to C.

Currently, NFPA 1977 standard does not account for the presence of additional layers throughout the garment and only evaluates outer shells, where it would only be a single layer for a wildlands garment on the forearms and lower legs. Vital areas, including the chest, abdomen, and upper thighs, can be protected by as many as three or four layers when considering overlapping jackets, pants, and reinforcements such as pockets. Fabrics AI through CL can be thought of as a replication of a firefighter's chest where an outer fire-resistant fabric and base layer t-shirt work in tandem together. This configuration is not an exact simulation as it does not accurately portray how a garment fits across the body, which would influence the air gap distances between the two separate layers. However, it will provide a general trend of the enhancement in protection gained by including the base layer into protection value calculations and taking a holistic, systems-level approach to clothing

heat/flame protection testing. Finally, once an additional layer has been introduced, the difference in protection between the progressing weights of fabric reduces. The air gaps between the fabric layers and the additional fabric dominate the thinner fabrics, suggesting a point of diminishing return when considering higher fabric weights.

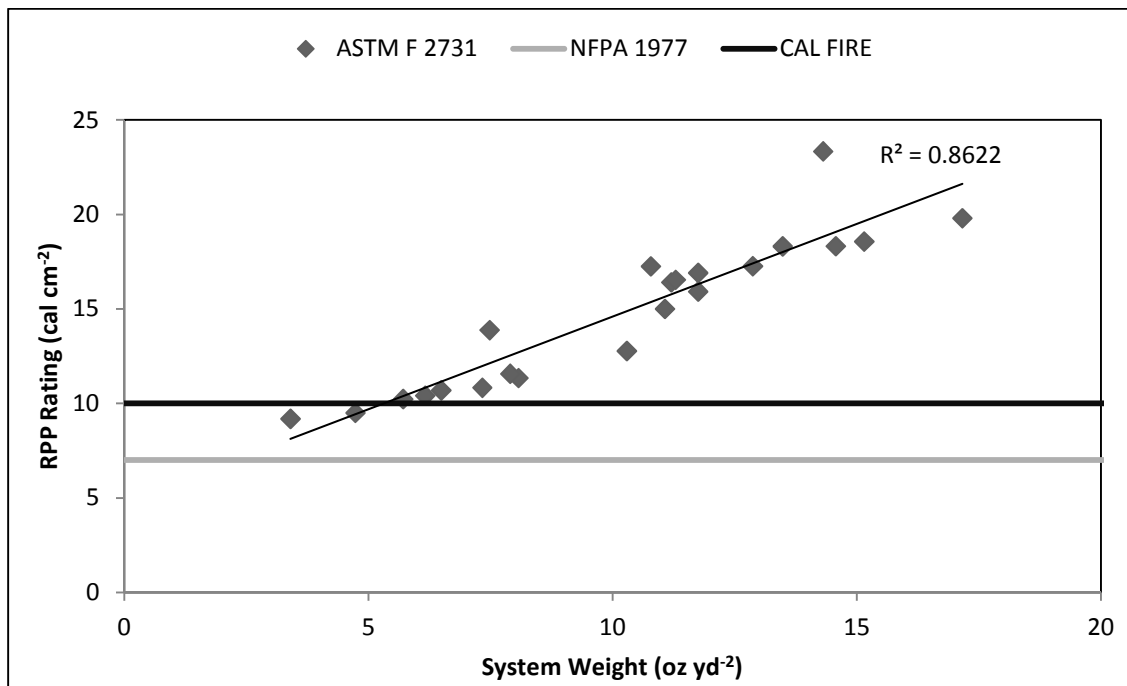


Figure 3- 4: RPP vs. Weight

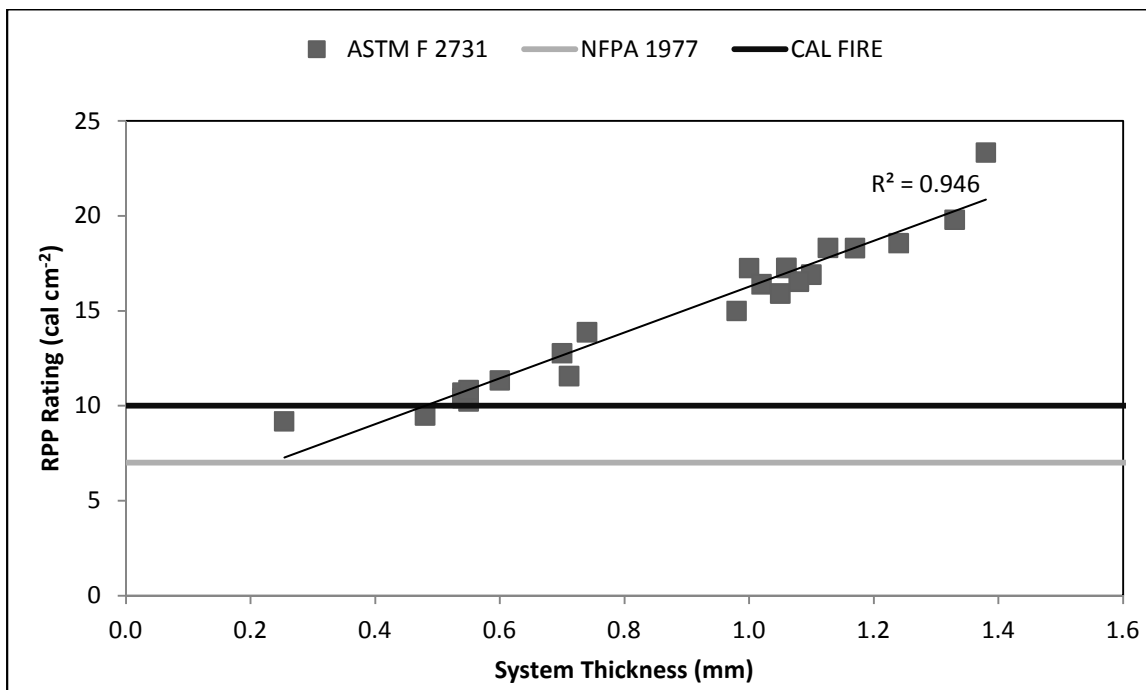


Figure 3- 5: RPP vs. Thickness

Figure 3- 4 and Figure 3- 5 demonstrate that thermal protection is directly related to weight and thickness with the latter providing the highest prediction correlation with RPP rating. These figures also show that in order for a fabric to pass the CAL FIRE criteria, it must possess a weight and thickness of at least 5 oz yd⁻² and 0.5 mm respectively.

3.5.1 Effect of Test Method

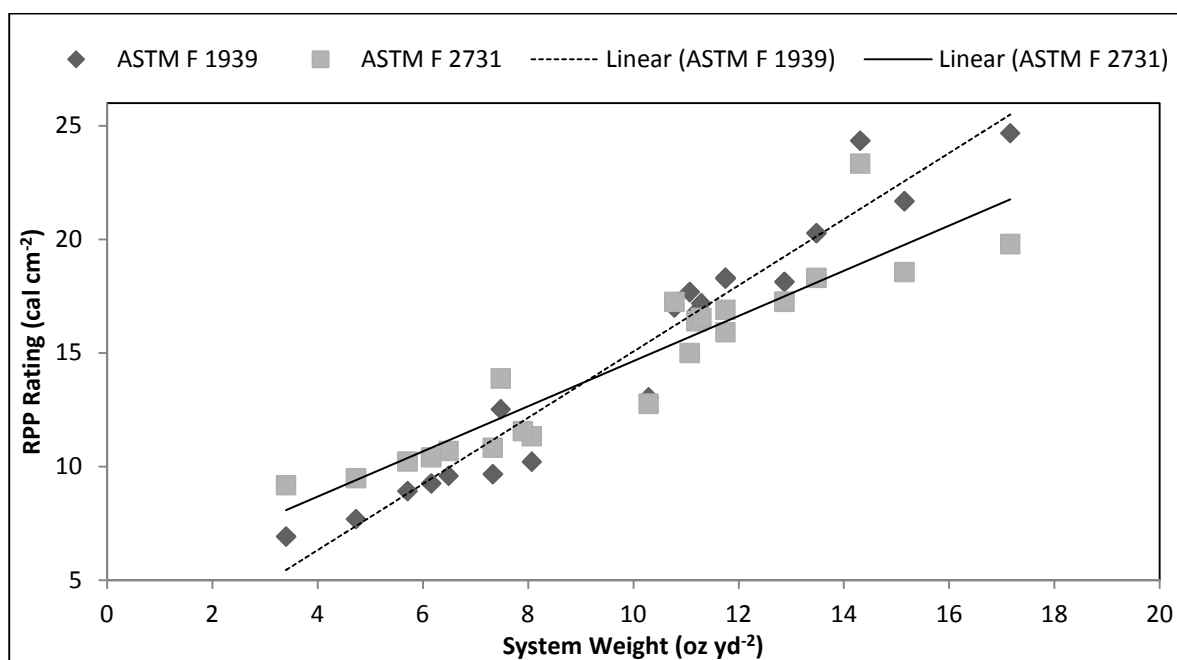


Figure 3- 6: Comparison of ASTM F 1939 & 2731 RPP vs. Weight

Figure 3- 6 compounds upon the statement made in Chapter 2 that the ASTM F 2731 platform supplies a higher heat flux than ASTM F 1939 until a certain weight is reached where heat saturation begins to lengthen the test exposure. It also shows that there is a significant jump in protection for multiple layer systems which reinforces the conclusion that the NFPA 1977 should consider base layers and double layers into their test methodology instead of solely focusing on single layer outer shells.

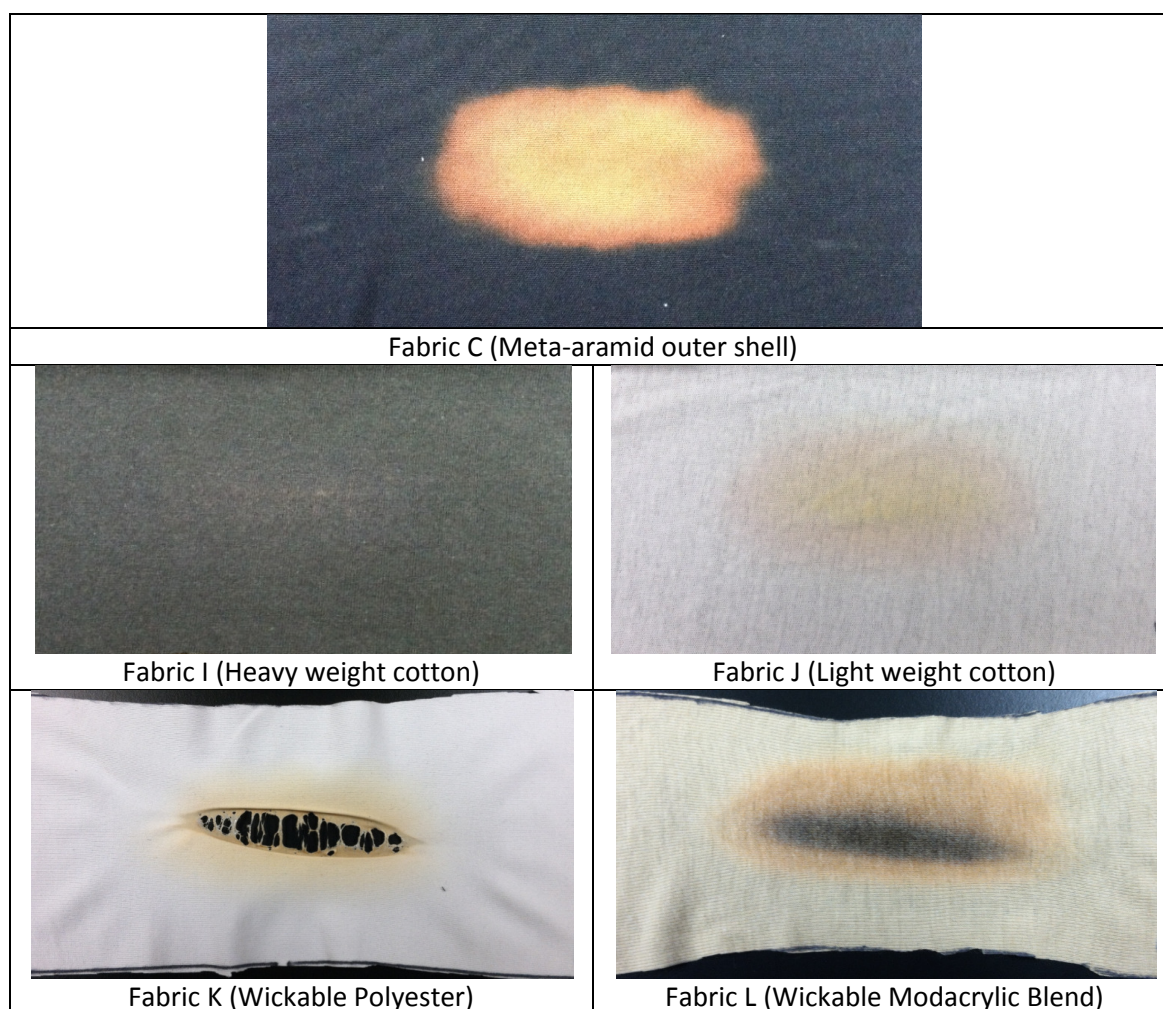


Figure 3- 7: Degradation of Fabrics when Tested by ASTM F 1939 Method

Figure 3- 7 illustrates the comparison between four base layer fabrics when tested in conjunction with outer shell fabric C and exposed to 21 kW m^{-2} (ASTM F 1939) until a second degree burn was reached. A good deal of qualitative data can be gathered from analyzing these degradation mechanisms. Both cotton samples changed color slightly with no change to flexibility or texture. The polyester samples melted and had breakthrough

where the heat intensity was strongest. Melting is an undesirable trait as droplets of melted polymer adhering to a firefighter's skin may result in an increased number of burns and greater difficulty for removal. Slight shrinkage was also present in the polyester material where shrinkage within a garment can dramatically alter the protection provided by decreasing the air layers between body and fabric thus reducing the insulation. It should be noted that degradation was only present in the standard 21 kW m^{-2} flux exposures and not the RME flux (7.1 kW m^{-2}), this includes the melting of the polyester which is of great concern to the firefighter community. However, the $500 \text{ }^\circ\text{F}$ oven test required by NFPA 1977 would have detected any weaknesses present in thermoplastic fabrics used [14]. Though polyester materials provide better wicking performance, it is still not recommended that these shirts be used until further research is performed. Bench level tests such as these are unable to detect or predict the effects that shrinkage would have on full scale garment. The modacrylic blend specimens changed color drastically and became very rigid to the point where any added flexural stress would cause the fabric to crack. Severe shrinkage was also evident in this fabric type after exposure.

3.6 Conclusions

This study showed that the major material factors controlling RPP are weight and thickness of clothing layers; higher fabric weight and additional layers of fabric increase predicted RPP by a great margin. The use of the RME exposure intensity in ASTM F 2731 leads to higher RPP values for single layer fabrics than the predicted values from ASTM F 1939. According to the data supplied by the ASTM F 2731 platform, all fabrics tested passed

the NFPA 1977 criteria and a minimum of approximately 5.0 oz yd⁻² weight would pass the CAL FIRE criteria of 10. It was shown that the presence of a base layer caused a large increase in RPP; however the specific type of material did not matter as much. Finally, it would be wise to use RPP tests at the RME exposure in conjunction with the 500 °F oven test in the attempt to eliminate thermoplastic materials that have the potential to melt when exposed to high temperatures.

CHAPTER 4: RADMAN™

4.1 Introduction

The wildlands firefighting environment is a complex and often unpredictable one. The conditions in which the firefighters operate can range anywhere from 14-81% in relative humidity and 63-91 °F in temperature [15]. However, with the exception of rare and intense situations, firefighters characteristically perform their duties a relatively safe distance from the flame front and only require protection from mild to moderate levels of radiant heat. This heat flux range in which the workers are operating under has been the topic of recent research with findings placing the most common working environments within a 5-10 kW m⁻² flux span [9]. Current test methods used to evaluate thermal protection for wildland firefighting personal protective equipment (PPE) implement a heat flux exposure of 21 kW m⁻² which is much higher than what recent research has established as the upper heat flux limit to what can be reasonably expected to see out in the field [7, 14]. This reduction in flux exposure creates a number of issues that must be addressed before it can be used in testing.

In addition to an inaccurate representation of the wildlands firefighting environment, the research methods being currently used for thermal protection evaluation all exist on a bench level scope. This approach is useful in providing a general idea of how a fabric would respond in the field use but is unable to account for all variables that exist within a garment such as fit, fabric layering, air gaps, and reinforcements like pockets and reflective trim. Bench level testing methods implement a standard air gap spacing (0.09 inch) [11] however this distance is not applicable to areas with large air spaces near the abdomen or where the fabric is in direct contact with the skin like at the shoulders. The current standard also only requires the testing of the outer shell fabric which ignores the base layers the firefighters wear in conjunction such as a t-shirt and undergarment. A more realistic garment scale test platform dressed exactly like a firefighter that is capable of mimicking the human physiological responses to thermal exposures that are applicable to a wildlands fire environment would greatly benefit the firefighting community.

4.2 Need for Radiant Man

Radiant Man (RadMan™) was developed in order to rectify the number of issues with current bench level test methods. Research into thermal protection provided by garments has shown that the air layer between skin and clothing is a major factor in the insulation from intense heat. The manner in which clothing naturally drapes across the body creates varying air layer thicknesses in every region which is impossible to replicate on the bench level scale where a static spacing is applied. Areas such as the shoulders where the garment is in direct contact with the skin or the abdomen where the garment is free flowing

cannot be directly simulated with this standard air spacing in bench level testing which only considers that a person is wearing a single layer of protective clothing [31]. The issue is exacerbated further when considering multi-layer systems with additional air gaps between clothing such as added base layers or the overlapping region between jacket and pants. The current standard [14] used for certifying wildlands PPE only requires the outer shell to be tested. By neglecting to account for the additional layers that are typically worn in practice, the data gained from required test methods is only supplying a piece of the puzzle to a much bigger picture for thermal protection. In addition to improving upon these deficiencies, a garment scale approach to wildland thermal dangers will also allow researchers to pinpoint weak spots in clothing construction by demonstrating precisely where burns are occurring. This is achieved by simulating the responses of a human while dressed exactly how a firefighter would be in the field. Locations such as the forearms and shins where only one layer of clothing is protecting the skin from a heat flux which should achieve burns faster and with more severity, as opposed to the waistline where at least three clothing layers are diminishing the heat flux that passes through to the skin.

The air gaps within the multiple garment layers are also of the utmost importance to thermal protection. Standard Radiant Protective Performance (RPP) testing [11] makes use of constant air spacing between sensor and fabric that is not applicable to the entire body. Areas where the garment is in contact with the body would not provide the same level of protection as those far away from the body. The variation between air spaces is impossible to predict without the use of a system built similarly to the human form. The same issue

arises when considering the air gaps between the fabric layers themselves. When testing on the RPP platform with multiple layers, which is not in compliance with the current standard, the fabrics are pressed directly against one another which is unrealistic, resulting in higher heat transfer through the system. These two misrepresentations of air layers in garments provide researchers with information that does not accurately portray the protection provided by PPE. This small difference between bench and garment scale testing may seem trivial but it is important to note that air is a superb insulator and provides a large portion of thermal protection provided by textiles.

PyroMan, a similar manikin system, is a widely accepted test method for the evaluation of thermal protection of garments when exposed to high heat fluxes and short duration scenarios such as a flash-over in structure fires. This recreation is achieved through the use of a series of eight propane flamethrowers to supply a heat flux of 84 kW m^{-2} for up to twelve seconds [26]. PyroMan makes use of a series of 122 PyroCal sensors to measure temperature and heat flux that unfortunately prove ineffective in the lower flux scenarios seen in wildland fires. The premise behind RadManTM is to simulate a realistic thermal environment that might be seen in the field for wildland firefighters. Current standards [11] for bench level test methods have set the upper limit for the thermal range at 21 kW m^{-2} which represents an “extraordinary” situation in which PPE would not be able to shield against for any extended period of time. A push for a lower Reasonable Maximum Exposure (RME) flux value of 7.1 kW m^{-2} has been made by a risk assessment study performed by CAL FIRE [7].

Investigative research into the limitations of sensors similar to the ones used in PyroMan have demonstrated that after an extended exposure to a heat source, a heat saturation effect takes place and drastically reduces the detected flux which increases the time until a burn is achieved which is the crux behind the entire test [32]. In order to obtain reliable data for lower heat flux exposures, the test platform must be able to account for the extended heat exposure times and mimic the human physiological response as best as technology will allow. While RadMan™ is fundamentally similar to its PyroMan counterpart, it has a number of key variations that allow the system to function in the lower flux environment.

4.3 RadMan™ Development

RadMan™ is a full size (male 50th percentile) manikin developed to evaluate the radiant protective performance of clothing systems in prolonged exposures to radiant heat. RadMan's heat source is from a lower flux heat panel that can either be gas or electrically powered and can supply between 5 to 21 kW m⁻² of flux with a water cooled heat shield used to block heat in between tests. RadMan™ is constructed from a metallic and fiber layered structure, in the attempt to simulate the human skin as much as possible. The RadMan™ skin surface is also entirely water-cooled to help combat heat saturation effects as well as simulate blood flow to further replicate human physiology. RadMan™ makes use of 70 RdF foil sensors due to the excellent response to flux when fixed to the manikin surface via epoxy and do not possess any issues with heat saturation.

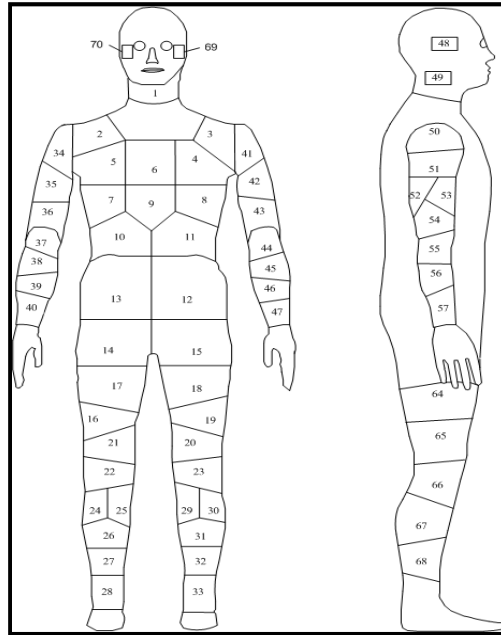


Figure 4- 1: RadMan™ Sensor Locations

While the sensors offer consistent readings, they do have a maximum temperature limitation of 100 °C before they break. The majority of the sensors are mounted to the front of the manikin while the remaining ones are on one side of the manikin. There are no sensors on the back surface. Due to the fact that the heat source is from a panel that provides a one directional flux, only one side of the manikin can be exposed at a time; thus, priority was given to the front and one side which can be assumed to be mirrored to the other. With this type of sensor configuration, standard test procedures may include a frontal exposure as well as an optional side exposure. The data during an experiment is sent to a data acquisition unit connected by a single Ethernet cord. Burn prediction is then calculated via the Henriques burn model [25]. RadMan™ is fully articulated, which allows the researcher to

place the manikin in any position necessary to evaluate how protection varies once the extremities are moved.

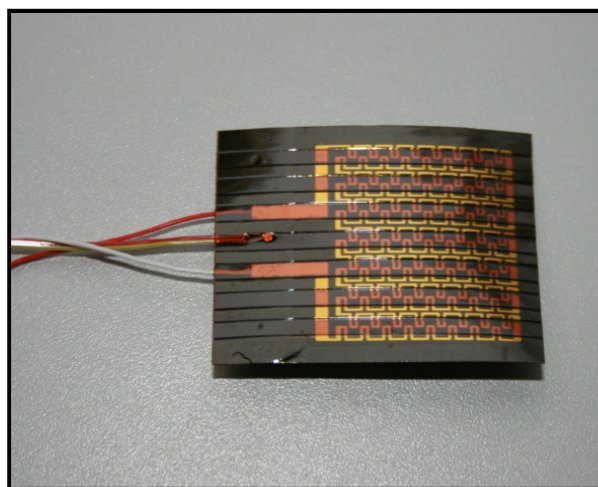


Figure 4- 2: RadMan™ RdF Foil Sensor

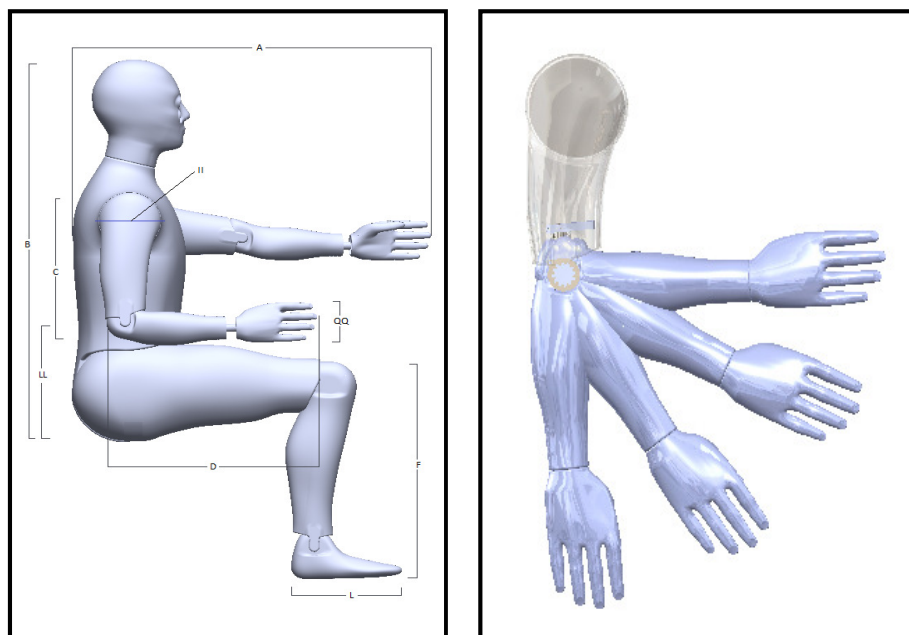


Figure 4- 3: RadMan™ Articulation

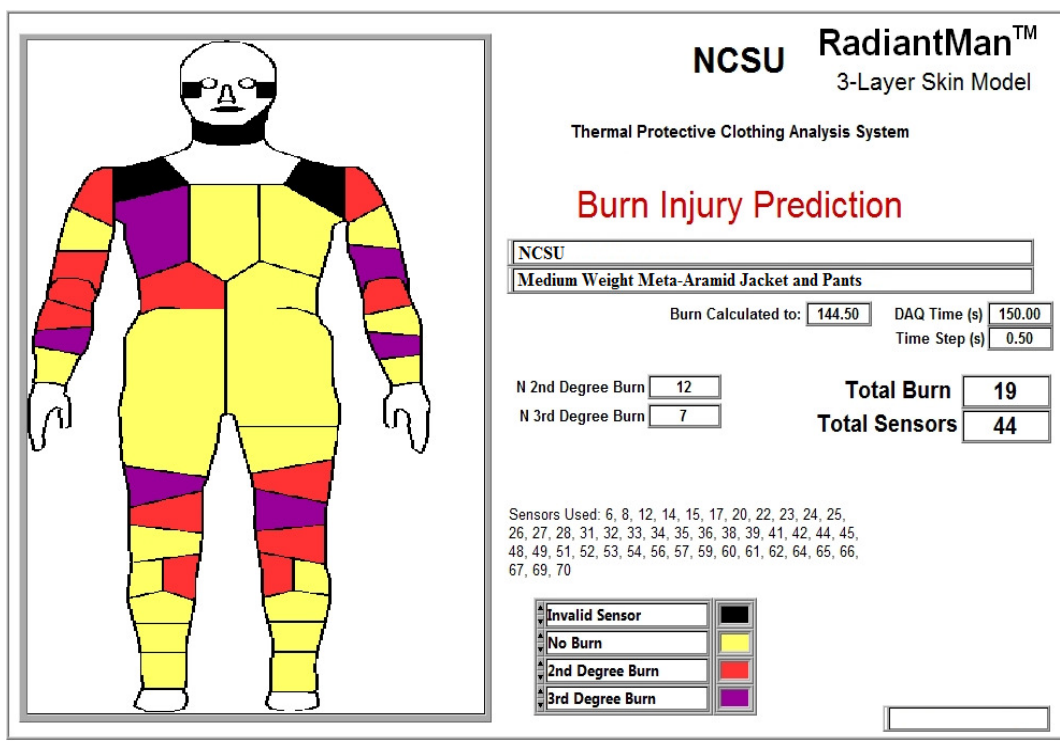


Figure 4- 4: RadMan™ Output

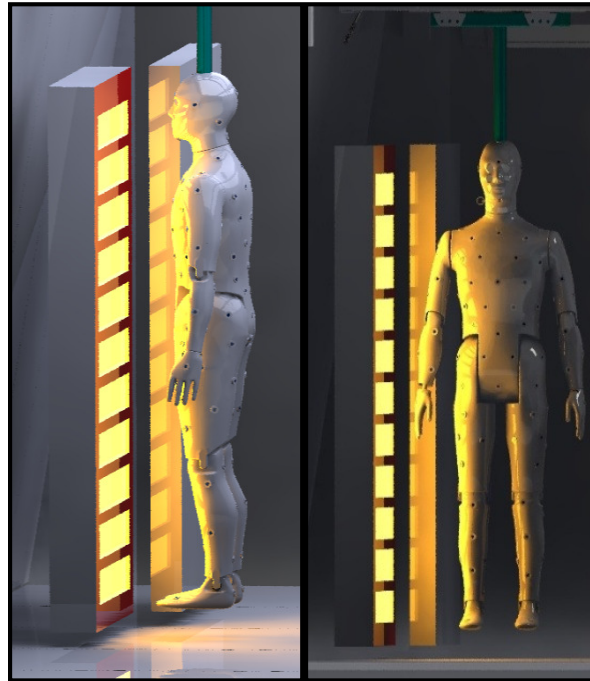


Figure 4- 5: RadMan™ Model

4.4 Results and Discussions

4.4.1 RadMan™ Sensor Validation

Before garment scale testing was conducted with the RadMan™ system, a series of experiments were carried out on the Stored Energy Tester platform [22] with a plate made out of the same material as RadMan™ using the RdF foil sensor. This was done in order to directly compare the results to the water cooled Schmidt-Boelter sensor utilized by the ASTM F 2731 test platform which has been proposed as a new RPP test methodology in Chapter 2. The bench level comparison tests included a range of varying weights as well as

woven and knit constructions. All fabric samples were composed of a 93% meta-aramid, 5% para-aramid, 2% antistatic fiber blend.

Table 4- 1: Bench Level Materials

ID	Construction	Weight (oz yd ⁻²)	Thickness (mm)
A	Plain Weave	3.4	0.25
B	Plain Weave	4.73	0.48
C	Plain Weave	6.49	0.54
D	Plain Weave	8.07	0.60
E	Plain Weave	10.29	0.70
F	Twill Weave	5.71	0.55
G	Twill Weave	6.16	0.54
H	Twill Weave	7.33	0.55
N	Twill Weave	7.90	0.71

The goal of these experiments was to demonstrate that RadMan's sensors produced very similar results to the test method deemed the most realistic representation of wildlands environments. Both test variations were exposed to a heat flux of 7.1 kW m⁻² and water cooled at blood temperature of 32.5 °C. Calibration between the two sensors is different. The RdF foil sensor was calibrated by exposing it to the RME flux for 10 seconds and taking the average over that time while the water cooled Schmidt-Boelter sensor was calibrated over 70 seconds and averaged over the last 60. Calibration was performed by shifting the manikin closer or further to the heat source in which very small adjustments resulted in large changes in recorded flux. The experiment was run until the computer software, dictated by the Henriques burn injury algorithm, determined a 2nd degree burn had been attained [25].

During testing, it was necessary to allow the sensor to return back to the starting 32.5°C temperature before another test could begin. This down time was usually between two to three minutes and was not necessary for standard ASTM F 2731 testing as the water flow is much higher allowing for faster cooling rates. Nonetheless, the end results were analogous with the RadMan™ plate.

Table 4- 2: RPP Rating of RadMan™ Sensor vs. ASTM F 2731 Sensor

Fabric Sample	RDF Foil Sensor	Schmidt-Boelter Sensor	Percent Difference
A	9.62	9.19	4.6%
B	10.24	9.50	7.5%
C	11.30	10.70	5.4%
D	12.17	11.35	7.0%
E	13.96	12.78	8.9%
F	10.92	10.23	6.5%
G	11.29	10.41	8.1%
H	11.56	10.84	6.5%
N	12.52	11.57	7.9%

4.4.2 RadMan™ Test Procedure

Once the sensors were proven to provide reasonable data, the focus was shifted to testing with the actual full scale RadMan™ system. The gas powered heat panel used as the heat source for the experiments measured 60 by 60.5 inches, 21.5 inches off the ground with a water cooled heat shield. The manikin was placed approximately four feet from the panel surface during testing and was adjusted accordingly depending upon calibration data. In order to calibrate RadMan™, the heat shield was removed from the heater to expose the manikin for a ten second window. The resulting flux values were averaged over that time span. The final calibration procedure provided a maximum RME flux over the surface. This calibration scheme offered a flux range of 4.0 to 7.1 kW m⁻² which allowed a test exposure of two and half minutes; enough to distinguish between different garment's protection values.

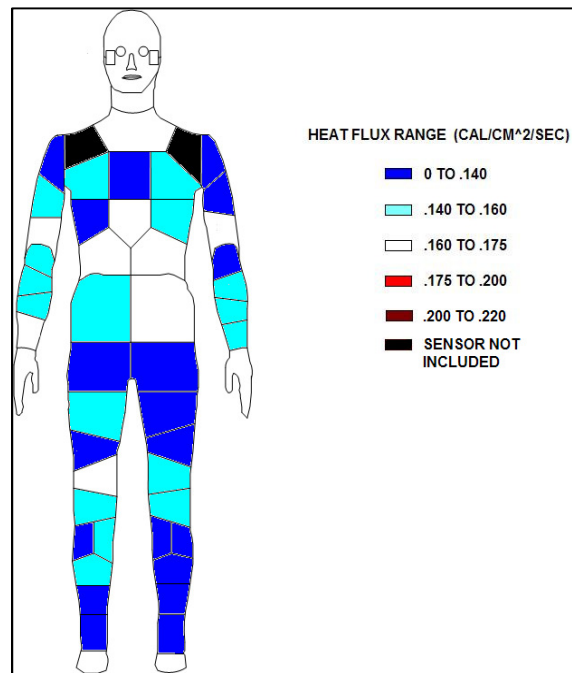


Figure 4- 6: RadMan™ Heat Flux Distribution

RadMan™ was designed to have the water running through its system to be similar to the same temperature of blood, approximately 32.5°C. However, due to the massive amount of raw heat (200 kW) produced by the heat panel, it was necessary to set the manikin's water temperature to 6 °C to enable the sensors to maintain temperatures below their 100 °C maximum cutoff long enough for usable data to be obtained, consequentially making the manikin's surface temp range from 20-25 °C. Ideally, once testing can commence at NCSU's facilities, the lower heat output from the electric powered panel will permit for increased water temperature.

The manikin was dressed in boxer briefs, t-shirt, helmet, PPE shirt, and pants. No gloves, socks or boots were worn because there are currently no sensors on the hands and feet. Each garment was exposed for a total of 150 seconds to a maximum of 7.1 kW m^{-2} over the entire front surface. After completion of each trial, the manikin was undressed and allowed to return back to a stable temperature. Each garment configuration was repeated 3 times. For the purpose of these experiments a total of 44 sensors on the front surface were utilized.

4.4.3 Test Materials

Experiments performed on the RadManTM test platform were carried out with a range of varying weights of meta-aramid garments, each washed three times in accordance to AATCC 135 [27]. Meta-aramid was selected as the fabric of choice because it is currently the standard fiber used in wildland firefighter garments. The USFS fabric is named differently because it is the current standard for most wildland firefighting configurations and is the control for these testing purposes. In terms of typical wildland firefighting garments, the fabrics selected for these experiments represent a wide range of weights in the attempt to evaluate if RadManTM is able to differentiate between garments with any reliability. All garments were exposed with a 6.0 oz yd^{-2} knit cotton base layer t-shirt beneath the outer shell PPE jacket. All garments were comprised of identical design with the exception of samples M, USFS, and DR which possessed minimal or additional reinforcements. In the context of this study, reinforcements refer to additional pockets, padding, and reflective trim. All

garments were sized to fit the RadMan™ manikin comfortably to properly replicate air layers between skin surface and clothing.



Figure 4- 7: RadMan™ Dressed in Wildland Fighting PPE

Table 4- 3: RadMan™ Materials

Identification	Jacket	Pants
A	3.3 oz yd ⁻² Meta-aramid Plain Weave	3.3 oz yd ⁻² Meta-aramid Plain Weave
M	6.0 oz yd ⁻² Meta-aramid Plain Weave	6.0 oz yd ⁻² Meta-aramid Plain Weave
USFS	5.8 oz yd ⁻² Meta-aramid Plain Weave	7.7 oz yd ⁻² Meta-aramid Twill Weave
D	7.5 oz yd ⁻² Meta-aramid Plain Weave	7.5 oz yd ⁻² Meta-aramid Plain Weave

Table 4-3 Continued		
DR	7.5 oz yd ⁻² Meta-aramid Plain Weave Extra Reinforcements	7.5 oz yd ⁻² Meta-aramid Plain Weave Extra Reinforcements
N	7.7 oz yd ⁻² Meta-aramid Twill Weave	7.7 oz yd ⁻² Meta-aramid Twill Weave
E	9.5 oz yd ⁻² Meta-aramid Plain Weave	9.5 oz yd ⁻² Meta-aramid Plain Weave
CD	6.0 & 7.5 oz yd ⁻² Meta-aramid Double Layer Plain Weave	6.0 & 7.5 oz yd ⁻² Meta-aramid Double Layer Plain Weave

4.5 Results and Discussion

RadMan's purpose is to provide information about protection from thermal radiant heat that cannot be found through the use of existing bench level test methods. Data such as where burns are occurring, and how large of an influence air layers hold over protection can be found from testing with RadMan™. A series of experiments were performed to assess the effects of exposure time (60, 90, 120, 150 seconds) at the maximum exposure intensity of 7.1 kW m⁻². Figure 4- 8 demonstrates the progression of burns predicted by the RadMan™ system at a range of time intervals. The highlighted regions in the far left portion indicate pockets which provide additional protection from radiant heat, which is illustrated by showing that protection on the left side is superior to the right due to the additional upper left torso pocket (Figure 4- 8). No burns were predicted in the lower torso area due to the overlapping jacket, pants, pockets, and underwear base layerings which provide a vast improvement in protection over a single outer shell layer. The data images on the right are color coded; white means there are no sensors, black means that sensor was removed from

burn prediction calculations, yellow means no burn was received, red means a 2nd degree burn was received, and purple means a 3rd degree burn was received. This qualitative examination of RadMan™ provides a wealth of information that may prove invaluable to researchers of wildland garments.

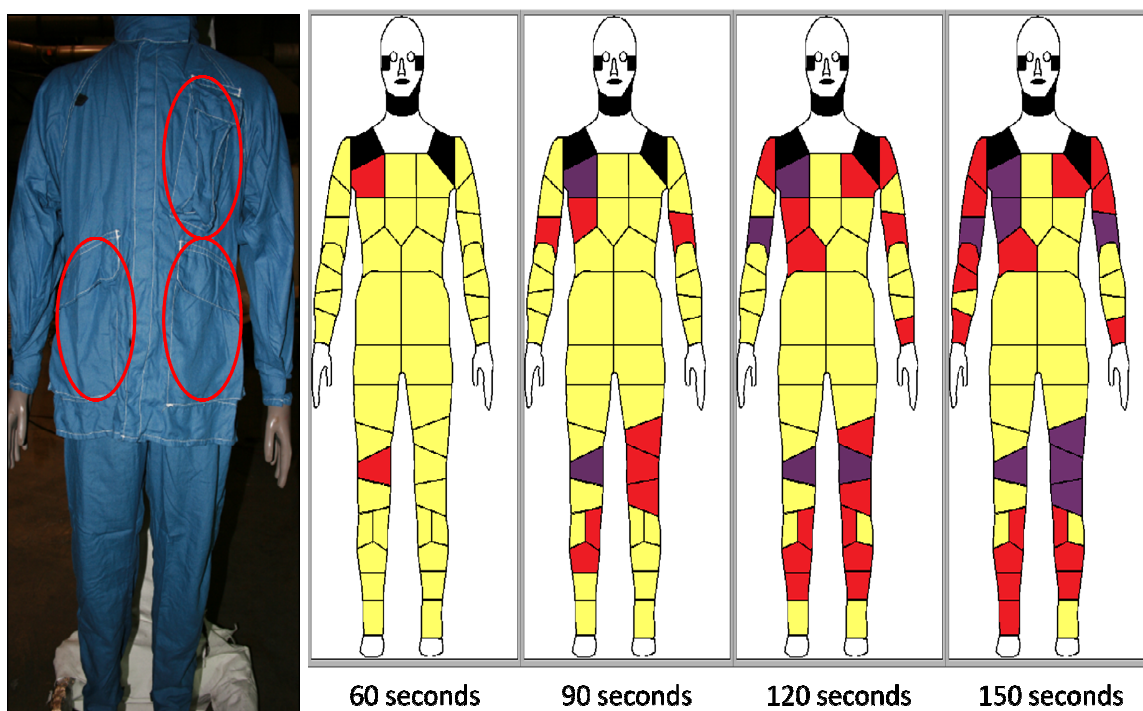


Figure 4- 8: Garment A Composite Image Time Progression

The following figures (9-12) demonstrate RadMan's ability to differentiate between varying weights of garments at increasing time-steps in the attempt to establish an optimum exposure time that provides the most usable data. The values indicate the percentage of

burns over the surface area of regions occupied by sensors (back, head, hands, and feet not included in total percentage) that predicted a 2nd or 3rd degree burn. The percentages were calculated by measuring the surface area that each sensor represents. This method provides a loose representation of the percentage of the portion from the front being burned which is easier to grasp than an arbitrary percentage of number of sensors burned. The data columns in Figures 9-12 are ordered by weight of garment.

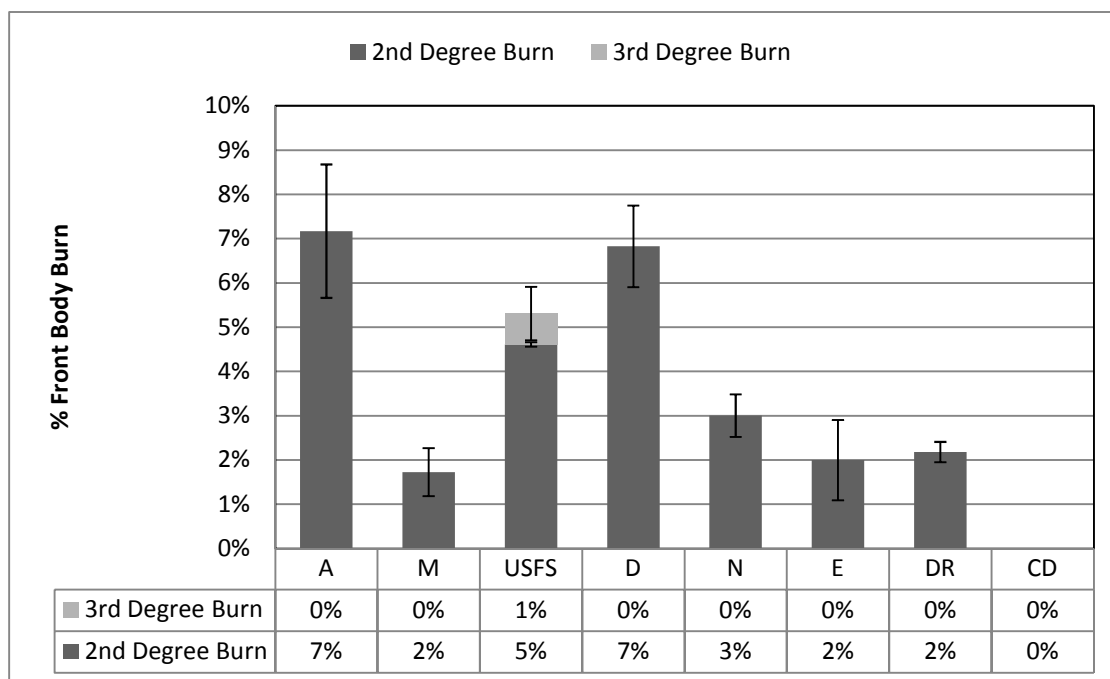


Figure 4- 9: RadMan™ Burn Data for Percentage of Front Body Burns at 60 Second Time Interval

The protection provided by garments is evident at about the 60 second mark where we start to see RadMan™ experiencing burns across the front surface during the garment testing. However, the data gathered at this time possesses such low percentage of burns and high standard deviations that no real conclusions about the garments can be made. In these cases, without any unaccounted for variables such as garment construction or additional pockets and reflective trim, the heaviest fabric provided the highest amount of protection. Figure 4- 9 reveals that not enough data has been collected at this time interval (60 seconds) to realistically differentiate between garments.

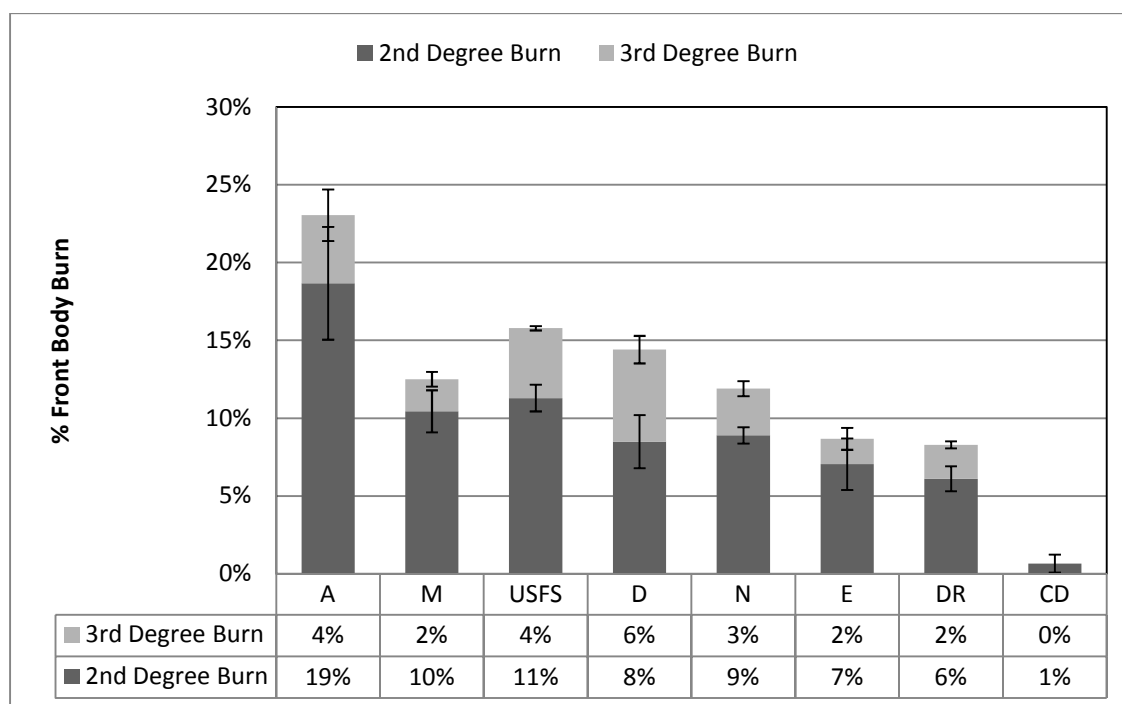


Figure 4- 10: RadMan™ Burn Data for Percentage of Front Body Burns at 90 Second Time Interval

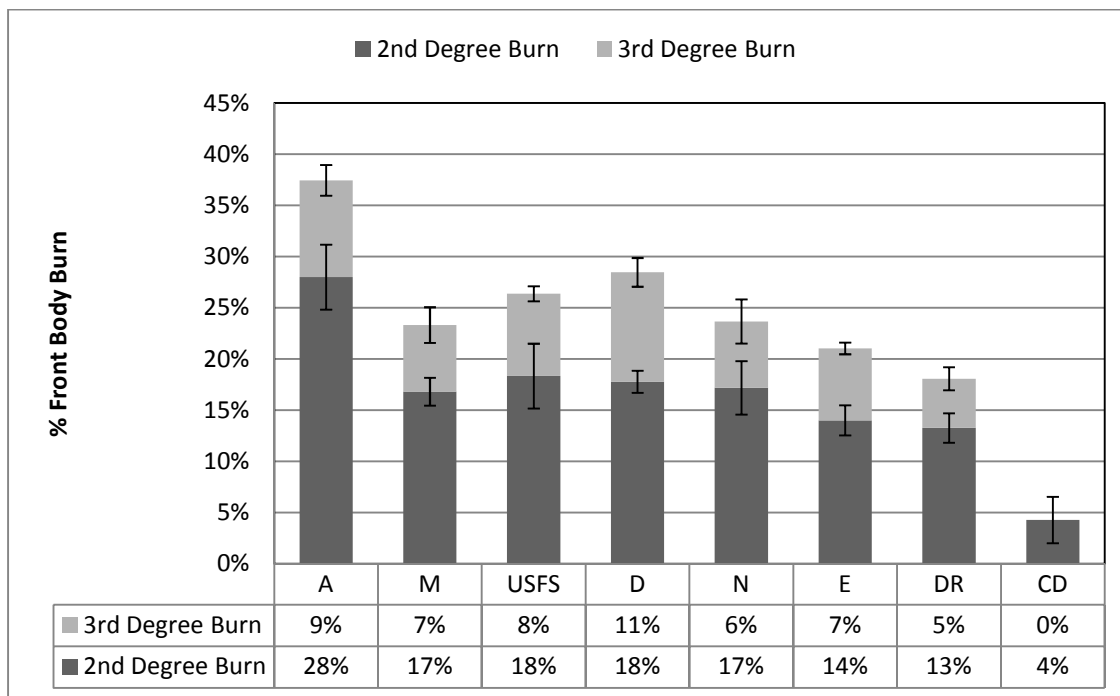


Figure 4- 11: RadMan™ Burn Data for Percentage of Front Body Burns at 120 Second Time Interval

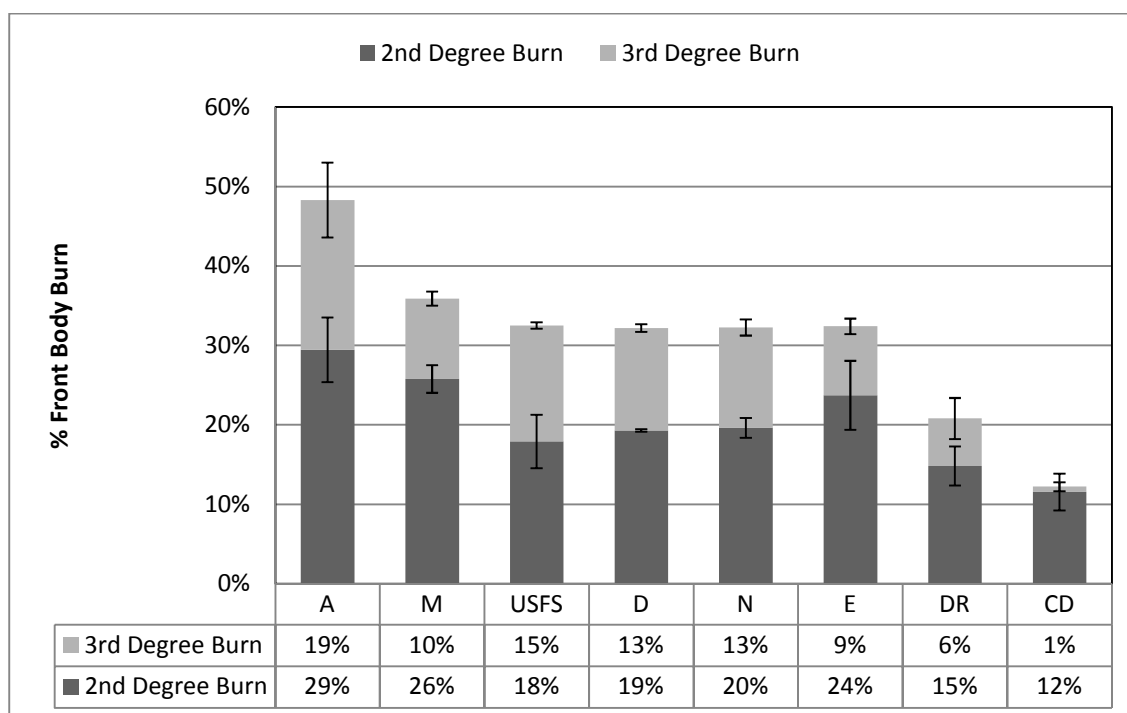


Figure 4- 12: RadMan™ Burn Data for Percentage of Front Body Burns at 150 Second Time Interval

As the exposure time increases, the differentiation between each garment becomes more prominent and the protection rankings begin to follow a more logical trend in relation to their respective weights. When the exposure time reaches 150 seconds, Figure 4- 12 looks as expected, where amount of burn injury decreases as garment weight increases. At this time interval, many of the garments are also statistically significant from one another. The concept behind RadMan™ is to point out differences in garments that bench level tests are not able to. In regards to a bench level experiment, garment E would perform better than garment D. RadMan™ is able to take that narrative a step further. In Figure 4- 12, when

garment D is outfitted with additional reinforcements such as extra pockets and reflective trim (DR), it outperforms E by a great deal. The system is also able to quantify the importance of double layer system as evidenced by the vast improvement in CD over the other garment samples. The additional fabric and air trapped between layers provides a large enhancement to protection from radiant heat. It is this additional information that is collected by RadMan™ that make it such an intriguing test platform because it cannot be found using bench level test methods.

4.5.1 Effect of Garment Construction

Figure 4- 13 illustrates that RadMan™ differentiates between protection locally and with logical consistency; meaning that where there is an additional layer or reinforcement, the protection increases as a result. This is best exemplified by the comparison between garments D and DR, as well as D and CD. Garments D and DR are identical in fabric weight however DR possesses extra padding, pockets and reflective trim in many areas. These areas have been highlighted in Figure 4- 13 and demonstrate the augmentation to protection provided. The fairly severe burn percentages RadMan™ was displaying across the forearms and thighs in D no longer exist in DR due to the additions. The comparison between D and CD provides insight into the improvement in protection with the addition of an extra layer, both from the thickness and air trapped between fabrics. Both garments are constructed from the same fabric but the latter possesses additional reinforcements and as a result, the difference between the two is fairly large. Protection is substantially higher in the lower abdomen in every garment sample due to the overlapping fabrics as well as the extra air layer between manikin surface and fabric that does not exist in areas with smaller air distances such as the forearms and shoulders.

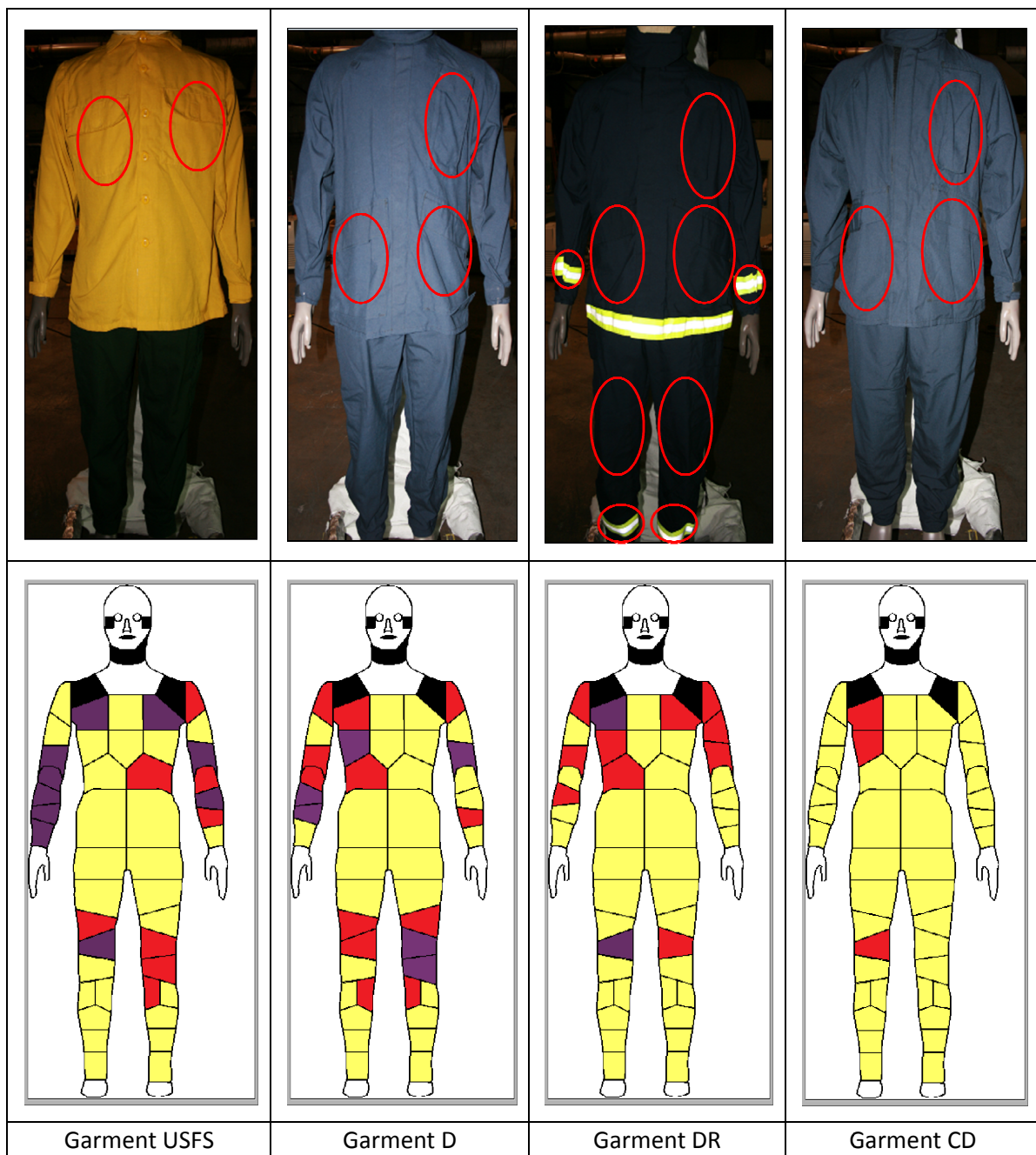


Figure 4- 13: Garment Construction Comparison

4.5.2 Garment Thermal Degradation

Each garment experienced some degree of thermal degradation after 150 seconds when exposed to the RME heat flux. This degradation usually manifested itself in the form of the burning off of the color dye within the fibers but it also melted the Velcro present in the garment construction of M. The base layers below the outer shells were not deteriorated at all. It has been well documented that meta-aramid fabrics shrink in the presence of intense thermal exposures due to their above average but not great thermal stability. Shrinkage of fabrics has the potential to mitigate the air layers between skin and fabric which will reduce protection. We do not believe this occurred in this specific set of experiments due to the relatively low exposure intensity but it is worth noting.

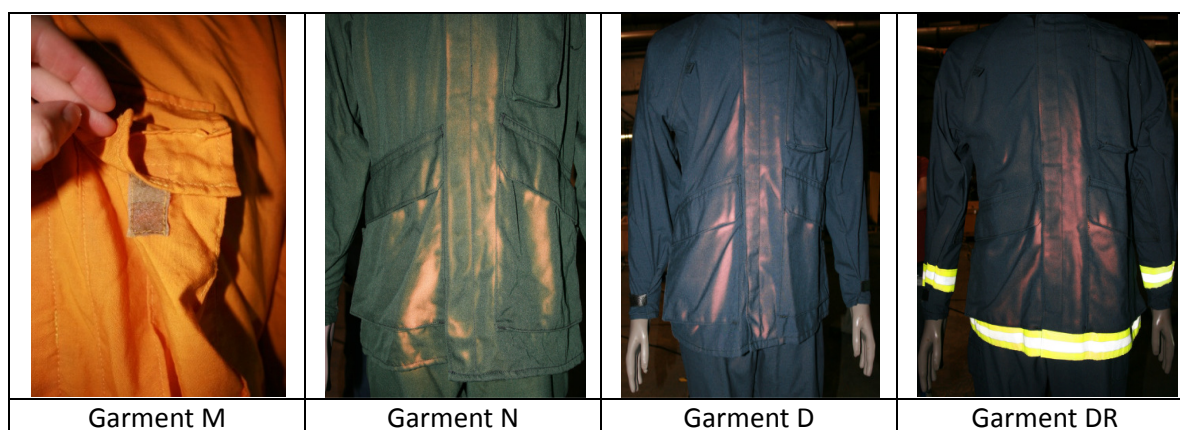


Figure 4- 14: Fabric Degradation after Thermal Exposure

4.5.3 Correlation between ASTM F 2731 RPP Rating and RadMan™

A comparison of bench level test fabrics to full scale garments of identical construction in Figure 4- 15 demonstrates an incredibly high correlation. This trend shows that the RadMan™ system closely mimics repeatable and valid bench level experiments very closely when all other variables such as alternate construction and reinforcements are removed from the equation.

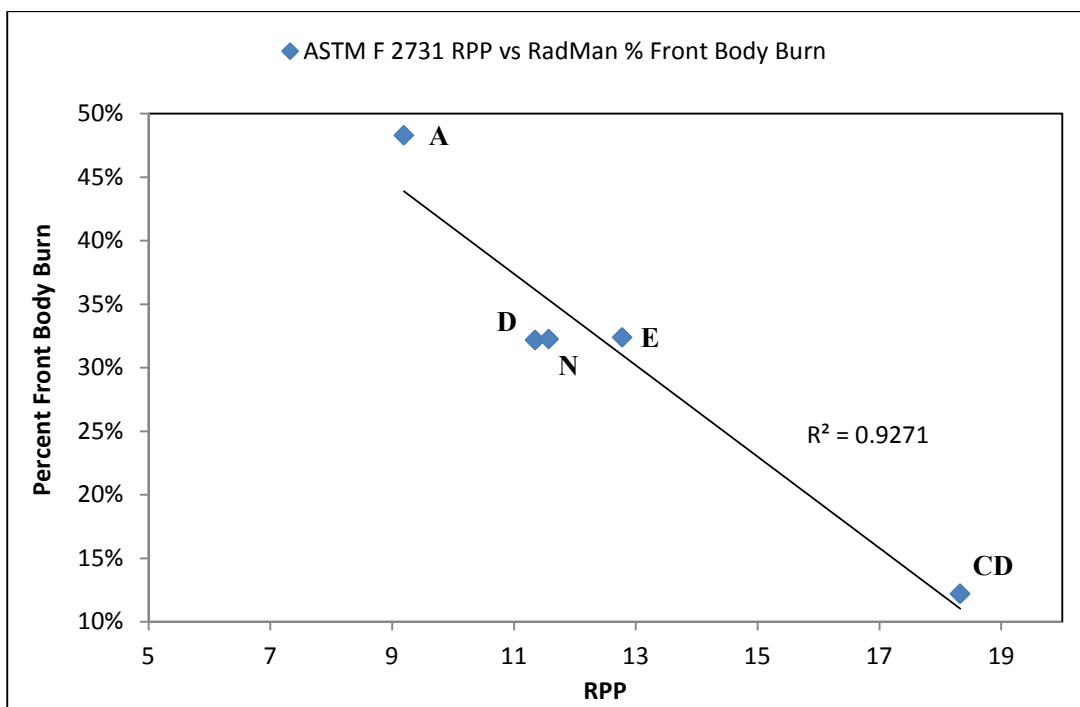


Figure 4- 15: Bench Level ASTM F 2731 RPP vs. Full Scale Front Body Burn % Comparison

4.6 Conclusions

This study has illustrated the development of a new full scale instrumented manikin system for evaluating wildland firefighter protective equipment. Preliminary testing with the RadMan™ system has demonstrated that the test platform is able to contribute additional data that bench level test methodologies are unable to provide. The correlation between bench scale and full scale results suggests the validity of the RadMan™ test methodology. Factors such as garment fit, air layers, and reinforcements are accounted for and displayed accordingly within the test results. The initial experiments established that a test exposure of at least 150 seconds is necessary in order to obtain useful information to effectively differentiate between garments. As with all comparisons between bench level and garment scale tests, such as sweating hot plate and sweating manikin, the difference between samples becomes blurred when tested on the full scale level. RadMan™ has the potential to be vital tool to evaluate protective garments worn by wildland firefighters.

CHAPTER 5: CONCLUSIONS AND RECOMMENDATIONS

Results from this research demonstrated the inability of ASTM F 1939 to function at RME flux levels as well as ASTM F 2731 platform's ability to correct these issues and operate effectively. This was done by illustrating the variation within ASTM F 1939 ranging from the prominence of heat flux in these longer test durations, lateral heating of fabric due to cooler unexposed regions functioning as heat sinks, as well as human error presence in the test method. The ASTM F 2731 platform's water cooled sensor and housing, sophisticated burn injury algorithm as well as the automated capabilities create an incredibly reliable test

method that is able to simulate a wildland fire and human physiological response as closely as technologically possible. It was established that the ASTM F 2731 apparatus was fully capable of differentiating between fabric weights and constructions as well as providing highly repeatable data. It was also shown that the major factors that influence thermal protection are weight and thickness of the fabric sample. The presence of an additional FR fabric or base layer improved the RPP rating by a vast margin which suggests that future standards in which fabrics are certified by should consider the possibility of incorporating multiple layer systems into their test methodology. The layering effects of additional thickness as well as trapped air between fabrics proved to be a large benefit in protection. The RadMan™ test platform was proven to possess a vast amount of potential for future research in regards to additional information not otherwise supplied by conventional bench level experiments. The consideration of full-scale effects such as garment fit, air layers, and reinforcements such as pockets and reflective trim proved to be large influences in overall protection. Finally, it was also shown that the correlation between full and bench scale experiments for directly comparable fabric specimens was very high which adds validity to the RadMan™ concept.

The large scale picture of this research is that a newer and more sophisticated test method has been developed for the evaluation of wildland firefighter garments. This test method has been proven to provide more realistic protection results that supplies higher RPP ratings for single layer fabric configurations which is the focus of the current NFPA 1977 standard which this study hopes to influence. These higher RPP ratings will ideally open the

door for lighter weight fabrics to be utilized in garments which will be more comfortable and less restrictive for firefighters which could lead to less heat stroke victims which is a rampant issue in today's firefighting work force.

5.1 Implications for Future Research

This research has brought about a variety of questions that, if answered, would prove beneficial to the wildlands community at large. An investigation into how the ASTM F 2731 apparatus differentiates between different fiber types such as polybenzimidazole (PBI) of a similar weight would prove the test method's worth further. The work done in this study will hopefully propel the ASTM F 2731 test platform into the NFPA 1977 standard as the main evaluation method of radiant protective performance. The majority of future research that stems from this study will hopefully advance the RadMan™ test platform into an accepted methodology. Additional experiments that further investigate how the full scale system functions under even heavier garment weights such as an FR fleece coat for the winter would undoubtedly help validate RadMan™. Finally, supplementary testing will allow researchers to obtain the optimal method for interpreting the data supplied by the manikin.

REFERENCES

[1] NWCG Safety and Health Working Team, "Wildland Firefighter Fatalities in the United States 1990 2006," 2007.

[2] G. Budd, J. Brotherhood, A. Hendrie, S. Jeffery, F. Beasley, B. Costin, W. Zhien, M. Baker, B. Hoschke, B. Holcombe, N. Cheney and M. Dawson, "Project Aquarius 13. The Thermal Burden of High Insulation and Encapsulation in Wildland Firefighter's Clothing," *International Journal of Wildland Fire*, vol. 7, pp. 207, 1997.

[3] L. Anderson and T. Petrilli, "Fire Shelter Overhaul," *Fire Chief*, pp. 59, 2003.

[4] *Loss of 19 firefighters in Arizona blaze 'unbearable', governor says.*
<http://www.cnn.com/2013/07/01/us/arizona-firefighter-deaths/index.html>, 2013.

[5] G. Budd, J. Brotherhood, A. Hendrie, S. Jeffery, F. Beasley, B. Costin, W. Zhien, M. Baker, B. Hoschke, B. Holcombe, N. Cheney and M. Dawson, "Project Aquarius 6. Heat Load from Exertion, Weather, and Fire in Men Suppressing Wildland Fires," *International Journal of Wildland Fire*, vol. 7, pp. 119, 1997.

[6] B. W. Butler and J. D. Cohen, "Firefighter Safety Zones: A Theoretical Model Based on radiative Heating," *International Journal of Wildland Fire*, vol. 8, pp. 73, 1998.

[7] C.F.P.P.E.W. Group, "Wildland Fire Fighting Hazard & Risk Assessment Draft Report," 2010.

[8] J. D. Cohen. Relating flame radiation to home ignition using modeling and experimental crown fires. *Canadian Journal of Forest Research* 34(8), pp. 1616-1626. 2004. DOI: 10.1139/X04-049.

[9] P. K. Raj. A review of the criteria for people exposure to radiant heat flux from fires. *J. Hazard. Mater.* 159(1), pp. 61-71. 2008. DOI: <http://dx.doi.org/prox.lib.ncsu.edu/10.1016/j.jhazmat.2007.09.120>.

- [10] D. Greenhalgh, "The Healing of Burn Wounds," *Dermatology Nursing*, vol. 8, pp. 13, 1996.
- [11] American Society for Testing and Materials, "ASTM F 1939 -08 Standard Test Method for Radiant Heat Resistance of Flame Resistant Clothing Materials with Continuous Heating," 2008.
- [12] National Fire Protection Association, "NFPA 1971: Standard on Protective Ensembles for Structural Fire Fighting and Proximity Fire Fighting," 2013.
- [13] National Fire Protection Association, "NFPA 2112: Standard on Flame-Resistant Garments for Protection of Industrial Personnel Against Flash Fire," 2013.
- [14] National Fire Protection Association, "NFPA 1977: Standard on Protective Clothing and Equipment for Wildland Fire Fighting," 2011.
- [15] G. Budd, J. Brotherhood, A. Hendrie, S. Jeffery, F. Beasley, B. Costin, W. Zhien, M. Baker, B. Hoschke, B. Holcombe, N. Cheney and M. Dawson, "Project Aquarius 4. Experimental bushfires, suppression procedures, and measurements," *International Journal of Wildland Fire*, vol. 7, pp. 99, 1997.
- [16] P. K. Raj. Field tests on human tolerance to (LNG) fire radiant heat exposure, and attenuation effects of clothing and other objects. *J. Hazard. Mater.* 157(2-3), pp. 247-259. 2008. . DOI: <http://dx.doi.org/prox.lib.ncsu.edu/10.1016/j.jhazmat.2007.12.114>.
- [17] A. Sullivan, P. Ellis and I. Knight, "A Review of Radiant Heat Flux Models Used in Bushfire Applications," *International Journal of Wildland Fire*, vol. 12, pp. 101, 2003.
- [18] D. Packham and A. Pompe, "Radiation Temperatures of Forest Fires," *Australian Forest Research*, vol. 5, pp. 1-8, 1971.
- [19] National Wildfire Coordinating Group, "Wildland Fire Suppression Tactics Reference Guide," 1996.

- [20] A. M. Stoll and L. Greene C., "Relationship between pain and tissue damage due to thermal radiation," *Applied Physiology*, vol. 14, pp. 373-382, 1959.
- [21] R. Barker, H. Hamouda, I. Shalev and J. Johnson, "Review and Evaluation of Thermal Sensors for Use in Testing Firefighters Protective Clothing," *National Institute of Standards and Technology*, 1999.
- [22] American Society for Testing and Materials, "ASTM F 2731 - 10 Standard Test Method for Measuring the Transmitted and Stored Energy of Firefighter Protective Clothing Systems," 2010.
- [23] L. Deuser, R. Barker, A. Deaton and A. Shepherd, "Interlaboratory Study of ASTM F 2731, Standard Test Method for Measuring the Transmitted and Stored Energy of Firefighter Protective Clothing Systems," *NIOSH National Personal Protective Technology Laboratory*, 2011.
- [24] J. A. Weaver and A. M. Stoll, "Mathematical Model of Skin Exposed to Thermal Radiation," 1967.
- [25] F. C. Henriques, "Studies of Thermal Injury V. The Predictability and the Significance of Thermally Induced Rate Processes Leading to Irreversible Epidermal Injury," pp. 489-502, 1947.
- [26] American Society for Testing and Materials, "ASTM F 1930 Standard Test Method for Evaluation of Flame Resistant Clothing for Protection Against Fire Simulations Using an Instrumented Manikin," 2013.
- [27] American Association of Textile Chemists and Colorists, "AATCC 135 - Dimensional Changes of Fabrics after Home Laundering," 2012.
- [28] American Society for Testing and Materials, "ASTM E 177 Standard Practice for Use of the Terms Precision and Bias in ASTM Test Methods," 2013.

- [29] American Society for Testing and Materials, "ASTM F 1868: Standard Test Method for Thermal and Evaporative Resistance of Clothing Materials Using a Sweating Hot Plate," 2012.
- [30] National Interagency Fire Center, "National Fireline Handbook Appendix B Fire Behavior," pp. 59, 2006.
- [31] G. Song, "Clothing Air Gap Layers and Thermal Protective Performance in Single Layer Garment," *Journal of Industrial Textiles*, vol. 36, pp. 193-205, 2007.
- [32] G. Song, S. Paskaluk, R. Sati, E. M. Crown, J. D. Dale and M. Ackerman, "Thermal protective performance of protective clothing used for low radiant heat protection," *Textile Research Journal*, vol. 81, pp. 311, 2011.

APPENDIX

APPENDIX

A.1 Cumulative to Instantaneous Heat Flux Conversion

The calculation for the conversion of cumulative heat flux to instant heat flux in Figure 2-11 and Figure 2-12 to allow for direct comparisons between the data provided by the copper slug sensor of ASTM F 1939 and the Schmidt-Boelter sensor of ASTM F 2731 are as follows.

$$q' = \frac{m \times C \times dT}{dt \times A}$$

Appendix Equation 1

Where q' = Instantaneous heat flux (J cm^{-2})
 m = Mass (g)
 C = Specific heat ($\text{J g}^{-1} \text{ } ^\circ\text{C}^{-1}$)
 dT = Change in temperature ($^\circ\text{C}$)
 A = Area of sensor (cm^2)
 dt = Change in time (s)

A.2 Significant Difference of ASTM F 1939 and 2731

Appendix Table 1: Statistical Significant Difference Analysis of Both Test Platforms

Sample	ASTM F 1939					ASTM F 2731				
	B	C	D	N	E	B	C	D	N	E
B		99%	99%	99%	99%		99%	99%	99%	99%
C			99%	99%	99%			99%	99%	99%
D				99%	99%				95%	99%
N					99%					99%
E										